CD4 T cell responses to persistent *Borrelia burgdorferi* infection

By

ELIZABETH M. HAMMOND
DISSERTATION

Submitted in partial satisfaction of the requirements for the degree of

DOCTOR OF PHILOSOPHY

in

Immunology

in the

OFFICE OF GRADUATE STUDIES

of the

UNIVERSITY OF CALIFORNIA

DAVIS

Approved:

Nicole Baumgarth, Chair

Smita Iyer

Charles Bevins

Committee in Charge

2022

Abstract

In response to microbial infection, effector CD4 T cells must polarize appropriately in order to induce an effective inflammatory response that leads to elimination of invading pathogens. Since *Borrelia burgdorferi* (Bb), the spirochetal agent of Lyme disease, evades immune clearance in infected mice and humans, we wanted to explore the possibility that inappropriate CD4 T cell polarization may contribute to bacterial persistence. In response to Bb infection, CD4 T cell polarization is considered to be Th1 dominant as a result of early Type I IFN production. Additionally, IFNγ producing T cells have been associated with Lyme disease pathology, especially arthritis of the large joints. However, when we stimulated CD4 T cells from Bb infected mice *ex vivo* with a recombinant form of the Bb surface Ag Arthritis Related Protein (Arp), we were unable to detect the hallmark cytokine produced by Th1 cells, IFNγ. This prompted us to re-examine the polarization state of effector CD4 T cells throughout Bb infection by quantitative RT-PCR and flow cytometry. We were surprised to find only modest Th1 polarization as measured by expression of the Th1 lineage defining transcription factor, Tbet (*Tbx21*), and little to no induction of *Ifng*. This could not be explained by enhanced polarization to two other major T helper lineages, Th2 or Th17. Nor could it be explained by the migration of polarized CD4 T cells to a T cell effector site, the skin, as skin resident T cells also failed to polarize. Furthermore, we did not observe enhanced effector polarization in Arp-specific CD4 T cells, as identified by a novel I-A^b tetramer. Instead, Arp-specific CD4 T cells were skewed toward a T follicular helper (Tfh) phenotype, which provides the first direct evidence that antigen specific Tfh are generated in response to Bb infection. Our data support the hypothesis that Bb induces suboptimal CD4 T cell polarization, thus we propose effector CD4 T cell polarization as a novel target of Bb immune evasion.

Acknowledgements

I'd like to begin by thanking my mentor, Dr. Nicole Baumgarth. Dr. Baumgarth has guided every step of this dissertation work and helped me build a strong foundational knowledge of immunology. It has been an absolute privilege to work so closely with such an exceptional scientist and academic.

Next, I'd like to thank my Dissertation Committee members, Dr. Smita Iyer and Dr. Charles Bevins. Dr. Iyer has provided invaluable feedback on my work, and I sincerely appreciate her thoughtful and challenging questions that always keep me on my toes. Dr. Bevins has been an incredible source of moral support throughout my PhD, and has helped me appreciate just how cunning microbes like *Borrelia burgdorferi* can be.

I have also had the privilege of working with many exceptional students and technicians throughout my time in the Baumgarth lab. A special thank you goes to Kim Olsen, for always being willing to lend a hand, and for generously sharing your knowledge and experience with the *Borrelia burgdorferi* project. I'd like to also acknowledge Giang (Vuvi) Tran, Fauna Smith, Jonathan Lam, Rebecca Blandino, Sara Rosero, Antonio Cembellin Prieto, Emma Keller, Jean Luo, Sharmila Sambanthamoorthy, and former lab members Karen Tracy, Hannah Savage, Trang Nguyen, Wahed Firoz, Janna Johnson, Shivneel Ram, and Jaykumar Bhatt. Thank you all for your feedback, your dedication to science, and most of all, for being wonderful people to work with.

Finally, I'd like to thank my family for all the support they have provided over the years. First and foremost, thank you to my husband Jeff Eglinger, for all the sacrifices you've made to help me to achieve this goal. Thank you to my daughter Ingrid, for bringing so much joy into my life. And a huge thanks to

my mother, Judy, for providing child care when the COVID-19 pandemic upended all of our lives. Mom, Jeff, and Ingrid—this dissertation is dedicated to you.

Table of Contents

Chapter 1

CD4 T cell responses in persistent *Borrelia burgdorferi* infection

As published in Current Opinion in Immunology, *77*:102187 (2022)

1.1 Abstract

Infection of mice with *Borrelia burgdorferi* (Bb), a tick-transmitted spirochete and the pathogen that causes Lyme disease in humans, triggers CD4 T cell activation in secondary lymphoid tissues, from which they disseminate into various infected tissues. Despite their activation and the appearance of CD4 T cell-dependent antibody responses, Bb establishes persistent infection in natural Bb reservoir hosts in the absence of overt disease, raising the question of the effectiveness of the anti-Bb T cell responses. Reviewing the existing literature, we propose that CD4 T cells might constitute a host cell target of Bb-mediated immune evasion, rendering these cells ineffective in orchestrating effective inflammatory responses and in supporting highly functional Bb-specific antibody induction. Supporting the induction of more effective CD4 T cell responses may help overcome Bb persistence.

1.2 Introduction

Borrelia burgdorferi *sensu stricto* (Bb), a spirochetal bacteria transmitted by Ixodes ticks, is the causative agent of Lyme disease in incidental hosts such as humans, dogs, and horses [1,2]. The pathogen establishes persistent infections without causing much of any disease in reservoir hosts such as small rodents and birds. This allows feeding larval and nymphal ticks to acquire Bb continuously and thus to perpetuate Bb's life cycle [3,4]. Evolutionary adaptation must have imbued Bb with potent immune evasion mechanisms to enable persistence in these hosts. Indeed, known Bb immune evasion strategies include suppression of innate immune responses, such as inhibition of complement-mediated killing, as well as the dynamic regulation of outer surface protein expression to escape antibody-mediated immunity, among others [5]. Less is known, however, about immune evasion mechanisms that might render T cell-mediated immunity unable to clear infections in reservoir species. In this review, we summarize known functions of CD4 T cells in anti-Bb immunity. As we outline, the existing literature fails to provide evidence that fully functional CD4 T cell responses develop after Bb infection, suggesting that these cells may constitute an additional host cell target of Bb-mediated immune evasion strategies.

1.3 CD4 T cell responses to Bb infection

Studies with cell subset-deficient mice first indicated that T cells had little impact on the course of Bb infection, while B cells appeared critical for controlling Bb tissue burden [6,7]. αβTCR+ CD4 T cells were shown to be induced to Bb antigens (Ags) in a cognate manner [8,9], however, the specificity of these anti-Bb T cells are largely unknown. CD4 T cells were shown also to be activated in an Bb Ag-independent manner [10], possibly via T cell-intrinsic [11] or extrinsic [12] TLR2 signaling. Non-classical T cells, such as gdT cells also seem to play a role in anti-Bb defense [13]. The extent to which CD4 T cell activation to Bb infection is Ag-specific versus the result of bystander activation remains an important open question. Another unanswered question pertains to the extent to which anti-Bb CD4 T

cell responses control bacteria burden and/or drive inflammation-induced tissue damage. Lyme disease pathology is largely believed to be immune mediated [3,14], driving Lyme arthritis, carditis, and neuroborreliosis [15-17]. Yet, the presence of Bb in tissues can also induce tissue damage and inflammation directly [18,19], although this correlation is not always straightforward [20-22]. CD4 T cells provide some control for Bb tissue levels [23], likely via induction of Bb-specific IgG, perhaps explaining why in some studies CD4 T cells were shown to limit or resolve Bb-infection induced pathology, rather than to cause it [24,25].

1.4 Effector CD4 T cell responses to Bb infection

Effector CD4 T cells were shown to be activated in secondary lymphoid organs (SLOs) presumably by professional antigen presenting cells (APCs), presenting Bb antigens in the context of MHC II (**Fig. 1.1**). They egress from SLOs to home to inflamed tissues via the blood, where CD4 T cells specific for Outer surface protein (Osp)A of Bb have been found at very low frequencies in humans [26]. Once in tissues, CD4 T cells can secrete pro- and anti-inflammatory cytokines, modulating the local inflammatory response to the invading spirochetes (**Fig. 1.1**). In humans and arthritis-prone mouse models, CD4 T cell accumulation in joint tissues is largely correlated with disease pathology [26,27], including after adoptive T cell transfer into Rag-deficient mice [15,28]. However, the transfer of Bb-primed T cells from mice either infected or immunized with Bb had no effect on either disease severity or bacterial clearance in SCID mice [28], while the co-transfer of B and T cells, or the transfer of B cells alone led to improved control of Bb-induced pathology, suggesting a pivotal role for B cell-mediated disease resolution [15,28]. These results also indicated that CD4 mediated T cell help might not be required for the generation of disease-protective antibodies, raising questions about CD4 T cell helper functions in Bb infection.

CD4 T cell effector polarization during Bb infection

Th1 polarization CD4 T cell effector polarization has been studied mostly in the context of Lyme arthritis (LA). CD4 T cells isolated from Bb-infected mice and humans suffering from LA secrete the Th1-associated cytokine IFNγ when stimulated *in vitro* with sonicated Bb [10,29], with stronger IFNγ production by synovial fluid CD4 T cells than those isolated from blood [30]. IFNγ production by CD4 T cells was seen also in LA-susceptible C3H mice, whereas stronger IL-4 responses (the canonical Th2 response) were noted in disease-resistant BALB/c mice [8,31]. While CD4 responses in adult C3H mice seem to recapitulate aspects of LA in humans [32], arthritis-development after Bb infection in adult C3H mice represents an outlier among mice, caused by a genetic defect that leads to the accumulation of DAMPs in infected joints [33]. Neither natural reservoir species such as *Peromyscus leucopus*, nor other laboratory mouse strains show overt signs of disease [34].

It remains unclear whether enhanced IFNγ production in LA is a result, or the cause of Bb-induced arthritis. Enhanced Th1 polarization and IFNγ production in disease-resistant BALB/c mice had no effect on the induction of arthritis [35], and genetic ablation of IFNγ in disease-susceptible C3H mice did not reduce arthritis severity [36]. Indeed, IFNγ producing CD4 T cells were essential for resolution of Bb-induced carditis, presumably via modulation of cardiac macrophage functions [24]. Furthermore, an additional blockade of TNFα signaling in IFNγ deficient mice exacerbated rather than relieved arthritis [37], and blockade of IL12 signaling via antibody treatment enhanced Bb tissue burden and arthritis severity [38], an effect, however, seen also in B and T cell deficient SCID mice [39]. A role for inflammatory CD4 T cells in limiting bacterial burden was demonstrated further in mice lacking the anti-inflammatory cytokine IL-10 [40] or lacking regulatory T cells [41]. These mice showed reduced Bb tissue burden, but also significantly enhanced arthritis severity and infiltration of joint tissues by Th1-polarized CD4 T cells [27]. As there are cellular sources of IFNγ other than CD4 T cells (macrophages, NK cells, CD8 T cells, B cells), further limiting a clear understanding of CD4 Th1 polarization versus IFNγ production and the effects on Bb infection outcome.

A potential mechanism of Th1 induction during Bb infection is the observed early generation of type I IFN [42,43], known drivers of Th1 polarization in viral infections [44]. Indeed, type I IFN production in response to *Streptococcus* spp. and *Helicobacter pylori*, examples of other extracellular bacterial infections, were shown to support host protection [45]. Canonical induction of type I IFN is triggered by endosomal TLR stimulation. Yet, type I IFN induction in Bb infection is produced independently of the TLR adaptor molecules MyD88 and TRIF [42,46], implicating other pathogen associated molecular pattern recognition receptors (PRRs), such as cytosolic nucleic acid sensors, as possible mediators of type I immunity [47]. Bacterial-derived nucleic acids can activate cytosolic PRRs, such as cGAS-STING and NOD-like receptors (NLRs), which initiate a type I IFN response [48-50]. Although macrophages efficiently phagocytose and degrade Bb [51], escape from the macrophage phagolysosome by some Bb may activate cytosolic PRRs [52]. Alternatively, cytosolic PRRs might be activated by host mitochondrial or nuclear DNA following Bb infection-induced cellular damage [53]. Further studies are needed to understand the mechanism of type I IFN induction by Bb, and its possible role in driving Th1 polarization.

Th2 polarization Early studies suggested that Th2 polarization could prevent inflammatory disease in Bb-infected BALB/c mice [8,54]. Consistent with this notion, Th2 skewing via mercury treatment ameliorated arthritis severity in C3H mice, despite delayed bacterial clearance [55]. However, C57BL/6 mice deficient in either IL-4 or IL-5 signaling showed enhanced rather than reduced resistance from Bb infection [56]. CD4 Th2 polarization does not appear to be strongly induced in response to Bb infection. Yet, a hallmark of Th2 effector responses, eosinophilia, has been described in Bb infected *Peromyscus leucopus* mice [57], as well as in cutaneous [58,59] and cardiac [60] Lyme Borreliosis patients. Whether this eosinophilia is the outcome of Th2-polarized CD4 T cell responses, however, and whether it can modulate infection outcome, has yet to be determined.

Th17 polarization Production of IL17 by CD4 T cells has been associated with protective immunity to extracellular bacterial and fungal infections [61]. However, in Bb infection Th17 responses may contribute to Lyme disease development in humans [62-64]. Consistent with these studies, Bb-infected IFNγ deficient C3H mice responded to antibody-mediated blockade of IL-17 with reductions in LA severity [65]. In mice with intact IFNγ signaling, however, deletion of IL-17 or IL-17R had no effect on the course of Bb infection [66,67], and the observed IL17 production might not even be derived from CD4 T cells [68].

Taken together, existing literature on CD4 effector responses to Bb have left no clear picture on the extent to which polarized effector CD4 T cells are induced and how they contribute to anti-Bb immunity (**Fig. 1.2**). While Th1 polarization has been observed particularly in the context of LA, the effects of CD4 T cells on the control of infection and contribution to or inhibition of inflammatory diseases associated with Bb infection appears complex. When considering that Bb establishes persistent, non-resolving infections in mice, the apparent lack of effective anti-Bb CD4 T cell effector induction may identify these cells as potential host cell targets of Bb-employed immune evasion strategies.

1.4 Helper CD4 T cell responses to *Borrelia burgdorferi* infection

Interaction of primed CD4 T cells with antigen-activated B cells in the T-B border zone of SLO's initiates T-dependent (TD) B cell responses, and also polarizes CD4 T cells to the T follicular helper (Tfh) cell state (**Fig. 1.2**). Tfh express the master transcriptional regulator Bcl6, upregulate the follicular homing chemokine receptor CXCR5, the inducible co-stimulator (ICOS), as well as programmed cell death (PD)-1 [69], all facilitating enhanced T-B interactions. This supports Ig class-switch recombination (CSR) from IgM to IgG and the development of two distinct B cell responses: an immediate and rapid differentiation

of cells into short-lived plasma blasts in the extrafollicular medullary compartment, a response that can also be initiated independent of T cell help; and the establishment of germinal centers (GCs) following the migration of Tfh and B cells into the follicle, a response that is dependent on CD4 T cells [70]. Inside the follicle, CXCR4+ GC Tfh support extensive B cell proliferation. Competition for T cell help is considered a main driver of selection of those B cells expressing the highest affinity antigen receptor.

The development of activated ICOS+ CXCR5+ CXCR4+/- CD4 Tfh in LNs but not the spleen of Bb-infected mice has been demonstrated [71,72], consistent with studies showing that the lack of T cell help in CD40L-deficient mice resulted in a sharp decline in Bb-specific IgG [73]. Furthermore, TD CSR of anti-Bb antibodies during infection was demonstrated by its absence in mice lacking CD40L [71,73]. There was also strong evidence for fulminant extrafollicular B cell responses in the LNs of Bb infected mice within 10 days of infection, as evidenced by the accumulation of CD138+ plasma blasts and plasma cells in the medullary cord areas of LNs, and rapid and transient increases in the numbers of antibody-secreting cells [72,74]. CD4 T cells isolated from LNs of Bb infected mice were able to provide strong help for B cell differentiation into plasma cells, but were less effective in supporting B cell proliferation [23], perhaps suggesting functional skewing of the CD4 T cell response in Bb infected mice towards support for extrafollicular responses. In Bb infection models were splenic involvement was noted, depletion of marginal zone (MZ) B cells via treatment with integrin-blocking antibodies led to reductions in Bb-specific IgG responses and, somewhat surprisingly given MZ B cell responses are largely considered to be induced independent of CD4 T cells, reduced frequencies of activated splenic CD4 T cells [75].

Despite the presence of Tfh and TD antibody responses in Bb-infected mice, multiple lines of evidence suggest that the TD B cell response to Bb is either not fully induced and/or not fully functional. First,

despite a need for CD40L expression for maximal anti-Bb IgG induction, there was no difference in the course of Bb infection in CD40L-/- mice compared to controls and serum from CD40L-/- mice provided the same level of passive protection as Bb-infected controls [73]. Similar findings were made with serum from mice lacking MHCII and/or CD4 T cells [76]. Second, although GCs are formed within about 2 weeks after Bb infection, they rapidly collapse over the next two weeks, with Tfh and GC B cells disappearing with similar kinetics [23,71,72]. This explains, at least in part, the transient nature of antibody-affinity maturation following Bb infection [23] and the absence of both memory B cells and long-lived bone marrow plasma cells (LLPCs), two hallmarks of TD GC responses [71]. Third, immune sera from TCRβ/δ gene-targeted mice proved equally efficacious to those from controls in providing passive protection from Bb challenge, although arthritis resolution in SCID mice was achieved only with transfer of control sera [7], further underscoring the limited effects of T cells on the quality and/or magnitude of the B cell response to Bb.

The mechanisms that render TD B cell responses ineffective for clearing Bb infections are likely multifactorial and include, to name but one example, the dynamic modulation of Borrelia surface antigen expression over the course of infection [3,5]. However, the failure of sustained GC is expected to significantly impact the quality of the TD B cell response. Unravelling the mechanisms causing these failures of the adaptive immune response will be critical for the devising prophylactic and therapeutic strategies that can overcome the immune response limitations seen after Bb infection.

1.6 Are CD4 T cells a host cell target of Bb mediated immune evasion?

It is well understood that CD4 T cell activation is critically affected by the cytokine milieu in which they are primed. In addition to cytokine signals provided by dendritic cells, tissue-derived inflammatory signals can also directly stimulate T cell fates [77]. Recent *in vitro* studies showed that stimulation of

CD4 T cells with Bb lysate-pulsed dendritic cells resulted in an exuberant differentiation of cells with a Tfh phenotype. The authors suggested, however, that these cells were in a "transient activation state", and required stimulation with pro-inflammatory cytokines such as IL1b and IL18 for effective differentiation into polarized effectors [78]. Given the robust appearance of Tfh-like CD4 T cells after Bb-infection *in vivo* [23,71,72], and a potentially ineffective polarization of CD4 T cells towards a robust effector state during subclinical infection (summarized above), aberrant inflammatory signals in SLO's induced to Bb infection, as indicated by a deterioration of the LNs architecture with loss of discrete T and B cell zones [74], might prevent the induction of CD4 T cells with appropriate functionalities. This could mean that CD4 T cells are not dispensable for controlling Bb infection, as suggested by early studies [6,7], but rather that during Bb infection CD4 T cell responses are suppressed such that their elimination has little effect on the course of Bb infection, precisely because they are non-functional.

1.7 Conclusion

Available studies indicate that Bb infection induces effector and helper CD4 T cell responses that are not fully functional, providing a possible explanation while early studies with T cell-deficient mice failed to demonstrate an impact of T cells on the course of Bb infection in mice. Yearly rates of Lyme disease have risen sharply over the last two decades, a trend likely to be enhanced by climate change and a wider distribution of the tick-vectors. There is an urgent need to expand the tools and models available to study the effects of Bb on adaptive immunity, especially the neglected area of Bb-induced T cell and TD B cell responses, to gain a better understanding of what could constitute effective immunity to this important pathogen. Existing data point to opportunities for identifying novel regulators of T cell responses during chronic infections.

1.8 Dissertation Outline

As previously stated, there are significant gaps in our understanding of how CD4 T cells are activated and polarized in response to Bb infection, and what roles these subsets have in host protection. The first aim of this dissertation is to provide a more comprehensive characterization of CD4 T cell functionality throughout early and late Bb infection. In chapter 2, I determined the effector and helper T cell polarization state of activated CD4 T cells in secondary lymph organs, blood, and the skin of Bb-infected mice at various times after infection by measuring the induction of key transcriptional regulators and effector cytokines. In chapter 3, I describe the identification of an immunogenic CD4 T cell epitope for the arthritis-related protein (Arp) of Bb. Using Arp peptide-MHC II tetramers I then analyzed Bb-specific CD4 T cell responses by flow cytometry and assessed their polarization state during Bb infection. My results indicate robust Tfh differentiation in lymph nodes rapidly after Bb infection but at best weak Th1 effector CD4 T cell polarization among both total activated CD4 T cells as well as those specific for Arp. For the first time, I have demonstrated that CD4 T cells can undergo antigen-specific activation and expansion in response to Bb in C57BL/6 mice. Taken together my data show that Bb infection induces CD4 T cell effector and helper responses that do not appear to contribute substantially to bacterial clearance, identifying CD4 T cells as potential host cell targets of Bb-induced immune evasion.

1.9 References

1. Steere AC, Strle F, Wormser GP, Hu LT, Branda JA, Hovius JW, Li X, Mead PS: **Lyme borreliosis**. *Nat Rev Dis Primers* 2016, **2**:16090.
2. Fritz CL, Kjemtrup AM: **Lyme borreliosis**. *Journal of the American Veterinary Medical Association* 2003, **223**:1261-1270.
3. Radolf JD, Caimano MJ, Stevenson B, Hu LT: **Of ticks, mice and men: understanding the dual-host lifestyle of Lyme disease spirochaetes**. *Nat Rev Microbiol* 2012, **10**:87-99.
4. Brunner JL, LoGiudice K, Ostfeld RS: **Estimating Reservoir Competence of Borrelia burgdorferi Hosts: Prevalence and Infectivity, Sensitivity, and Specificity**. *Journal of Medical Entomology* 2008, **45**:139-147.
5. Bockenstedt LK, Wooten RM, Baumgarth N: **Immune Response to Borrelia: Lessons from Lyme Disease Spirochetes**. *Curr Issues Mol Biol* 2021, **42**:145-190.
6. Fikrig E, Barthold SW, Chen M, Chang CH, Flavell RA: **Protective antibodies develop, and murine Lyme arthritis regresses, in the absence of MHC class II and CD4+ T cells**. *The Journal of Immunology* 1997, **159**:5682-5686.
7. McKisic MD, Barthold SW: **T-cell-independent responses to Borrelia burgdorferi are critical for protective immunity and resolution of lyme disease**. *Infect Immun* 2000, **68**:5190-5197.
8. Matyniak JE, Reiner SL: **T helper phenotype and genetic susceptibility in experimental Lyme disease**. *The Journal of Experimental Medicine* 1995, **181**:1251-1254.
9. Schaible UE, Kramer MD, Justus CW, Museteanu C, Simon MM: **Demonstration of antigen-specific T cells and histopathological alterations in mice experimentally inoculated with Borrelia burgdorferi**. *Infect Immun* 1989, **57**:41-47.
10. Infante-Duarte C, Kamradt T: **Lipopeptides of Borrelia burgdorferi outer surface proteins induce Th1 phenotype development in alphabeta T-cell receptor transgenic mice**. *Infection and Immunity* 1997, **65**:4094-4099.
11. Whiteside SK, Snook JP, Ma Y, Sonderegger FL, Fisher C, Petersen C, Zachary JF, Round JL, Williams MA, Weis JJ: **IL-10 Deficiency Reveals a Role for TLR2-Dependent Bystander Activation of T Cells in Lyme Arthritis**. *The Journal of Immunology* 2018, **200**:1457-1470.
12. Collins C, Shi C, Russell JQ, Fortner KA, Budd RC: **Activation of γδ T Cells by *Borrelia burgdorferi* Is Indirect via a TLR- and Caspase-Dependent Pathway**. *The Journal of Immunology* 2008, **181**:2392-2398.
13. Divan A, Budd RC, Tobin RP, Newell-Rogers MK: **γδ T Cells and dendritic cells in refractory Lyme arthritis**. *J Leukoc Biol* 2015, **97**:653-663.
14. Petzke M, Schwartz I: **Borrelia burgdorferi Pathogenesis and the Immune Response**. *Clin Lab Med* 2015, **35**:745-764.
15. McKisic MD, Redmond WL, Barthold SW: **Cutting Edge: T Cell-Mediated Pathology in Murine Lyme Borreliosis**. *The Journal of Immunology* 2000, **164**:6096-6099.
16. Lasky C, Pratt C, Hilliard K, Jones J, Brown C: **T cells exacerbate Lyme borreliosis in TLR2-deficient mice**. *Frontiers in Immunology* 2016, **7**.
17. Lünemann JD, Gelderblom H, Sospedra M, Quandt JA, Pinilla C, Marques A, Martin R: **Cerebrospinal Fluid-Infiltrating CD4+ T Cells Recognize Borrelia burgdorferi Lysine-Enriched Protein Domains and Central Nervous System Autoantigens in Early Lyme Encephalitis**. *Infection and Immunity* 2007, **75**:243-251.
18. Hyde JA: **Borrelia burgdorferi Keeps Moving and Carries on: A Review of Borrelial Dissemination and Invasion**. *Frontiers in Immunology* 2017, **8**.
19. Jutras BL, Lochhead RB, Kloos ZA, Biboy J, Strle K, Booth CJ, Govers SK, Gray J, Schumann P, Vollmer W, et al.: ***Borrelia burgdorferi* peptidoglycan is a persistent antigen in patients with Lyme arthritis**. *Proceedings of the National Academy of Sciences* 2019, **116**:13498-13507.

20. Zeidner NSS, B. S.; Dolan, M. C.; Piesman J: **An Analysis of Spirochete Load, Strain, and Pathology in a Model of Tick-Transmitted Lyme Borreliosis**. *Vector-Borne and Zoonotic Diseases* 2001, **1**:35-44.
21. Liu N, Montgomery RR, Barthold SW, Bockenstedt LK: **Myeloid differentiation antigen 88 deficiency impairs pathogen clearance but does not alter inflammation in Borrelia burgdorferi-infected mice**. *Infect Immun* 2004, **72**:3195-3203.
22. Donta ST, States LJ, Adams WA, Bankhead T, Baumgarth N, Embers ME, Lochhead RB, Stevenson B: **Report of the Pathogenesis and Pathophysiology of Lyme Disease Subcommittee of the HHS Tick Borne Disease Working Group**. *Frontiers in Medicine* 2021, **8**.
23. Elsner RA, Hastey CJ, Baumgarth N: **CD4+ T cells promote antibody production but not sustained affinity maturation during Borrelia burgdorferi infection**. *Infect Immun* 2015, **83**:48-56.
24. Bockenstedt LK, Kang I, Chang C, Persing D, Hayday A, Barthold SW: **CD4+ T Helper 1 Cells Facilitate Regression of Murine Lyme Carditis**. *Infection and Immunity* 2001, **69**:5264-5269.
25. Nardelli DT, Cloute JP, Luk KHK, Torrealba J, Warner TF, Callister SM, Schell RF: **CD4+ CD25+ T Cells Prevent Arthritis Associated with Borrelia Vaccination and Infection**. *Clinical and Diagnostic Laboratory Immunology* 2005, **12**:786-792.
26. Meyer AL, Trollmo C, Crawford F, Marrack P, Steere AC, Huber BT, Kappler J, Hafler DA: **Direct enumeration of Borrelia-reactive CD4 T cells ex vivo by using MHC class II tetramers**. *Proceedings of the National Academy of Sciences* 2000, **97**:11433-11438.
27. Sonderegger FL, Ma Y, Maylor-Hagan H, Brewster J, Huang X, Spangrude GJ, Zachary JF, Weis JH, Weis JJ: **Localized Production of IL-10 Suppresses Early Inflammatory Cell Infiltration and Subsequent Development of IFN-γ–Mediated Lyme Arthritis**. *The Journal of Immunology* 2012, **188**:1381-1393.
28. Schaible UE, Wallich R, Kramer MD, Nerz G, Stehle T, Museteanu C, Simon MM: **Protection against Borrelia burgdorferi infection in SCID mice is conferred by presensitized spleen cells and partially by B but not T cells alone**. *International Immunology* 1994, **6**:671-681.
29. Yssel H, Shanafelt MC, Soderberg C, Schneider PV, Anzola J, Peltz G: **Borrelia burgdorferi activates a T helper type 1-like T cell subset in Lyme arthritis**. *The Journal of Experimental Medicine* 1991, **174**:593-601.
30. Gross DM, Steere AC, Huber BT: **T helper 1 response is dominant and localized to the synovial fluid in patients with Lyme arthritis**. *J Immunol* 1998, **160**.
31. Dong Z, Edelstein MD, Glickstein LJ: **CD8+ T cells are activated during the early Th1 and Th2 immune responses in a murine Lyme disease model**. *Infection and Immunity* 1997, **65**:5334-5337.
32. Heilpern AJ, Wertheim W, He J, Perides G, Bronson RT, Hu LT: **Matrix Metalloproteinase 9 Plays a Key Role in Lyme Arthritis but Not in Dissemination of *Borrelia burgdorferi***. *Infection and Immunity* 2009, **77**:2643-2649.
33. Bramwell KK, Ma Y, Weis JH, Chen X, Zachary JF, Teuscher C, Weis JJ: **Lysosomal β-glucuronidase regulates Lyme and rheumatoid arthritis severity**. *J Clin Invest* 2014, **124**:311-320.
34. Ma Y, Seiler KP, Eichwald EJ, Weis JH, Teuscher C, Weis JJ: **Distinct Characteristics of Resistance to *Borrelia burgdorferi*-Induced Arthritis in C57BL/6N Mice**. *Infection and Immunity* 1998, **66**:161-168.
35. Shanafelt M-C, Kang I, Barthold SW, Bockenstedt LK: **Modulation of Murine Lyme Borreliosis by Interruption of the B7/CD28 T-Cell Costimulatory Pathway**. *Infection and Immunity* 1998, **66**:266-271.
36. Brown CR, Reiner SL: **Experimental Lyme Arthritis in the Absence of Interleukin-4 or Gamma Interferon**. *Infection and Immunity* 1999, **67**:3329-3333.
37. Christopherson JA, Munson EL, England DM, Croke CL, Remington MC, Molitor ML, DeCoster DJ, Callister SM, Schell RF: **Destructive arthritis in vaccinated interferon gamma-deficient mice**

challenged with Borrelia burgdorferi: modulation by tumor necrosis factor alpha. *Clin Diagn Lab Immunol* 2003, **10**:44-52.
38. Anguita J, Persing DH, Rincon M, Barthold SW, Fikrig E: **Effect of anti-interleukin 12 treatment on murine lyme borreliosis**. *The Journal of Clinical Investigation* 1996, **97**:1028-1034.
39. Anguita J, Samanta S, Barthold SW, Fikrig E: **Ablation of interleukin-12 exacerbates Lyme arthritis in SCID mice**. *Infection and Immunity* 1997, **65**:4334-4336.
40. Brown JP, Zachary JF, Teuscher C, Weis JJ, Wooten RM: **Dual Role of Interleukin-10 in Murine Lyme Disease: Regulation of Arthritis Severity and Host Defense**. *Infection and Immunity* 1999, **67**:5142-5150.
41. Siebers EM, Liedhegner ES, Lawlor MW, Schell RF, Nardelli DT: **Regulatory T Cells Contribute to Resistance against Lyme Arthritis**. *Infect Immun* 2020, **88**.
42. Miller JC, Ma Y, Bian J, Sheehan KC, Zachary JF, Weis JH, Schreiber RD, Weis JJ: **A critical role for type I IFN in arthritis development following Borrelia burgdorferi infection of mice**. *J Immunol* 2008, **181**.
43. Petzke MM, Iyer R, Love AC, Spieler Z, Brooks A, Schwartz I: **Borrelia burgdorferi induces a type I interferon response during early stages of disseminated infection in mice**. *BMC Microbiol* 2016, **16**:29.
44. Crouse J, Kalinke U, Oxenius A: **Regulation of antiviral T cell responses by type I interferons**. *Nature Reviews Immunology* 2015, **15**:231-242.
45. Carrero JA: **Confounding roles for type I interferons during bacterial and viral pathogenesis**. *International Immunology* 2013, **25**:663-669.
46. Hastey CJ, Ochoa J, Olsen KJ, Barthold SW, Baumgarth N: **MyD88- and TRIF-independent induction of type I interferon drives naive B cell accumulation but not loss of lymph node architecture in Lyme disease**. *Infect Immun* 2014, **82**:1548-1558.
47. Cavlar T, Ablasser A, Hornung V: **Induction of type I IFNs by intracellular DNA-sensing pathways**. *Immunology & Cell Biology* 2012, **90**:474-482.
48. Liu N, Pang X, Zhang H, Ji P: **The cGAS-STING Pathway in Bacterial Infection and Bacterial Immunity**. *Frontiers in Immunology* 2022, **12**.
49. Petnicki-Ocwieja T, Kern A: **Mechanisms of Borrelia burgdorferi internalization and intracellular innate immune signaling**. *Frontiers in cellular and infection microbiology* 2014, **4**:175-175.
50. Watanabe T, Asano N, Kitani A, Fuss IJ, Chiba T, Strober W: **Activation of type I IFN signaling by NOD1 mediates mucosal host defense against Helicobacter pylori infection**. *Gut Microbes* 2011, **2**:61-65.
51. Benjamin SJ, Hawley KL, Vera-Licona P, La Vake CJ, Cervantes JL, Ruan Y, Radolf JD, Salazar JC: **Macrophage mediated recognition and clearance of Borrelia burgdorferi elicits MyD88-dependent and -independent phagosomal signals that contribute to phagocytosis and inflammation**. *BMC Immunology* 2021, **22**:32.
52. Woitzik P, Linder S: **Molecular Mechanisms of Borrelia burgdorferi Phagocytosis and Intracellular Processing by Human Macrophages**. *Biology* 2021, **10**:567.
53. Sok SPM, Ori D, Nagoor NH, Kawai T: **Sensing Self and Non-Self DNA by Innate Immune Receptors and Their Signaling Pathways**. *Crit Rev Immunol* 2018, **38**:279-301.
54. Rao TD, Frey AB: **Protective Resistance to Experimental Borrelia burgdorferi Infection of Mice by Adoptive Transfer of a CD4+ T Cell Clone**. *Cellular Immunology* 1995, **162**:225-234.
55. Ekerfelt C, Andersson M, Olausson A, Bergström S, Hultman P: **Mercury exposure as a model for deviation of cytokine responses in experimental Lyme arthritis: HgCl2 treatment decreases T helper cell type 1-like responses and arthritis severity but delays eradication of Borrelia burgdorferi in C3H/HeN mice**. *Clin Exp Immunol* 2007, **150**:189-197.
56. Zeidner NS, Schneider BS, Rutherford JS, Dolan MC: **Suppression of Th2 cytokines reduces tick-transmitted Borrelia burgdorferi load in mice**. *J Parasitol* 2008, **94**:767-769.

57. Schwanz LE, Brisson D, Gomes-Solecki M, Ostfeld RS: **Linking disease and community ecology through behavioural indicators: immunochallenge of white-footed mice and its ecological impacts**. *Journal of Animal Ecology* 2011, **80**:204-214.
58. Granter SR, Barnhill RL, Hewins ME, Duray PH: **Identification of Borrelia burgdorferi in Diffuse Fasciitis With Peripheral Eosinophilia: Borrelial Fasciitis**. *JAMA* 1994, **272**:1283-1285.
59. Colli C, Leinweber B, Müllegger R, Chott A, Kerl H, Cerroni L: **Borrelia burgdorferi-associated lymphocytoma cutis: clinicopathologic, immunophenotypic, and molecular study of 106 cases**. *Journal of Cutaneous Pathology* 2004, **31**:232-240.
60. Tavora F, Burke A, Li L, Franks TJ, Virmani R: **Postmortem confirmation of Lyme carditis with polymerase chain reaction**. *Cardiovascular Pathology* 2008, **17**:103-107.
61. Gaffen SL, Moutsopoulos NM: **Regulation of host-microbe interactions at oral mucosal barriers by type 17 immunity**. *Sci Immunol* 2020, **5**.
62. Strle K, Sulka KB, Pianta A, Crowley JT, Arvikar SL, Anselmo A, Sadreyev R, Steere AC: **T-Helper 17 Cell Cytokine Responses in Lyme Disease Correlate With Borrelia burgdorferi Antibodies During Early Infection and With Autoantibodies Late in the Illness in Patients With Antibiotic-Refractory Lyme Arthritis**. *Clinical Infectious Diseases* 2017, **64**:930-938.
63. Shen S, Shin JJ, Strle K, McHugh G, Li X, Glickstein LJ, Drouin EE, Steere AC: **Treg cell numbers and function in patients with antibiotic-refractory or antibiotic-responsive lyme arthritis**. *Arthritis & Rheumatism* 2010, **62**:2127-2137.
64. Gyllemark P, Forsberg P, Ernerudh J, Henningsson AJ: **Intrathecal Th17- and B cell-associated cytokine and chemokine responses in relation to clinical outcome in Lyme neuroborreliosis: a large retrospective study**. *Journal of Neuroinflammation* 2017, **14**:27.
65. Burchill MA, Nardelli DT, England DM, DeCoster DJ, Christopherson JA, Callister SM, Schell RF: **Inhibition of Interleukin-17 Prevents the Development of Arthritis in Vaccinated Mice Challenged with *Borrelia burgdorferi***. *Infection and Immunity* 2003, **71**:3437-3442.
66. Kuo J, Warner TF, Munson EL, Nardelli DT, Schell RF: **Arthritis is developed in Borrelia-primed and -infected mice deficient of interleukin-17**. *Pathog Dis* 2016, **74**.
67. Lasky CE, Jamison KE, Sidelinger DR, Pratt CL, Zhang G, Brown CR: **Infection of Interleukin 17 Receptor A-Deficient C3H Mice with Borrelia burgdorferi Does Not Affect Their Development of Lyme Arthritis and Carditis**. *Infection and Immunity* 2015, **83**:2882-2888.
68. Hansen ES, Johnson ME, Schell RF, Nardelli DT: **CD4+ cell-derived interleukin-17 in a model of dysregulated, Borrelia-induced arthritis**. *Pathogens and Disease* 2016, **74**:ftw084-ftw084.
69. Juno JA, Hill DL: **T follicular helper cells and their impact on humoral responses during pathogen and vaccine challenge**. *Curr Opin Immunol* 2021, **74**:112-117.
70. Baumgarth N: **The Shaping of a B Cell Pool Maximally Responsive to Infections**. *Annu Rev Immunol* 2021, **39**:103-129.
71. Elsner RA, Hastey CJ, Olsen KJ, Baumgarth N: **Suppression of Long-Lived Humoral Immunity Following Borrelia burgdorferi Infection**. *PLoS Pathog* 2015, **11**:e1004976.
72. Hastey CJ, Elsner RA, Barthold SW, Baumgarth N: **Delays and diversions mark the development of B cell responses to Borrelia burgdorferi infection**. *J Immunol* 2012, **188**:5612-5622.
73. Fikrig E, Barthold SW, Chen M, Grewal IS, Craft J, Flavell RA: **Protective antibodies in murine Lyme disease arise independently of CD40 ligand**. *The Journal of Immunology* 1996, **157**:1-3.
74. Tunev SS, Hastey CJ, Hodzic E, Feng S, Barthold SW, Baumgarth N: **Lymphoadenopathy during lyme borreliosis is caused by spirochete migration-induced specific B cell activation**. *PLoS Pathog* 2011, **7**:e1002066.
75. Belperron AA, Dailey CM, Booth CJ, Bockenstedt LK: **Marginal zone B-cell depletion impairs murine host defense against Borrelia burgdorferi infection**. *Infect Immun* 2007, **75**:3354-3360.
76. Fikrig E, Barthold SW, Chen M, Chang CH, Flavell RA: **Protective antibodies develop, and murine Lyme arthritis regresses, in the absence of MHC class II and CD4+ T cells**. *J Immunol* 1997, **159**:5682-5686.

77. Hu W, Troutman TD, Edukulla R, Pasare C: **Priming microenvironments dictate cytokine requirements for T helper 17 cell lineage commitment**. *Immunity* 2011, **35**:1010-1022.
78. Mandraju R, Jain A, Gao Y, Ouyang Z, Norgard MV, Pasare C: **MyD88 Signaling in T Cells Is Critical for Effector CD4 T Cell Differentiation following a Transitional T Follicular Helper Cell Stage**. *Infection and Immunity* 2018, **86**.

1.10 Figures

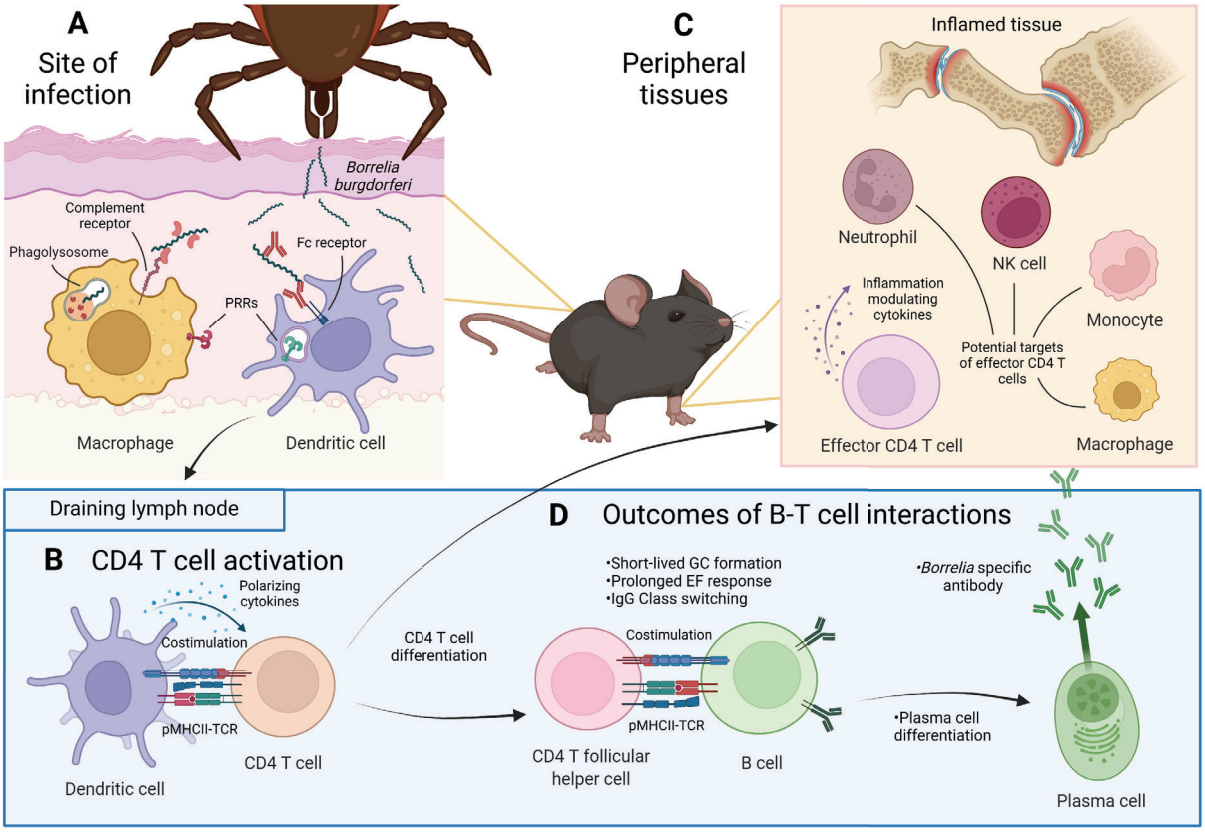

Figure 1.1: Summary of CD4 T cell responses to *Borrelia burgdorferi* (Bb) infection. A) Adult *Ixodes* sp. ticks transmit Bb spirochetes. Resident antigen-presenting cells phagocytose Bb in the context of local inflammatory signals. B) DCs migrate from the site of infection to the draining lymph node presenting Bb antigen to naïve CD4 T cells in the context of peptide-MCH II (pMHCII). APC-derived cytokines shape CD4 T cell polarization. C) Effector CD4 T cells migrate to Bb infected tissues to modulate inflammation by secreting anti-inflammatory cytokines (IL-10), or pro-inflammatory cytokines such as IFNγ. D) Bb-specific T follicular helper (Tfh) cells induce and regulate germinal center and extrafollicular B cell responses.

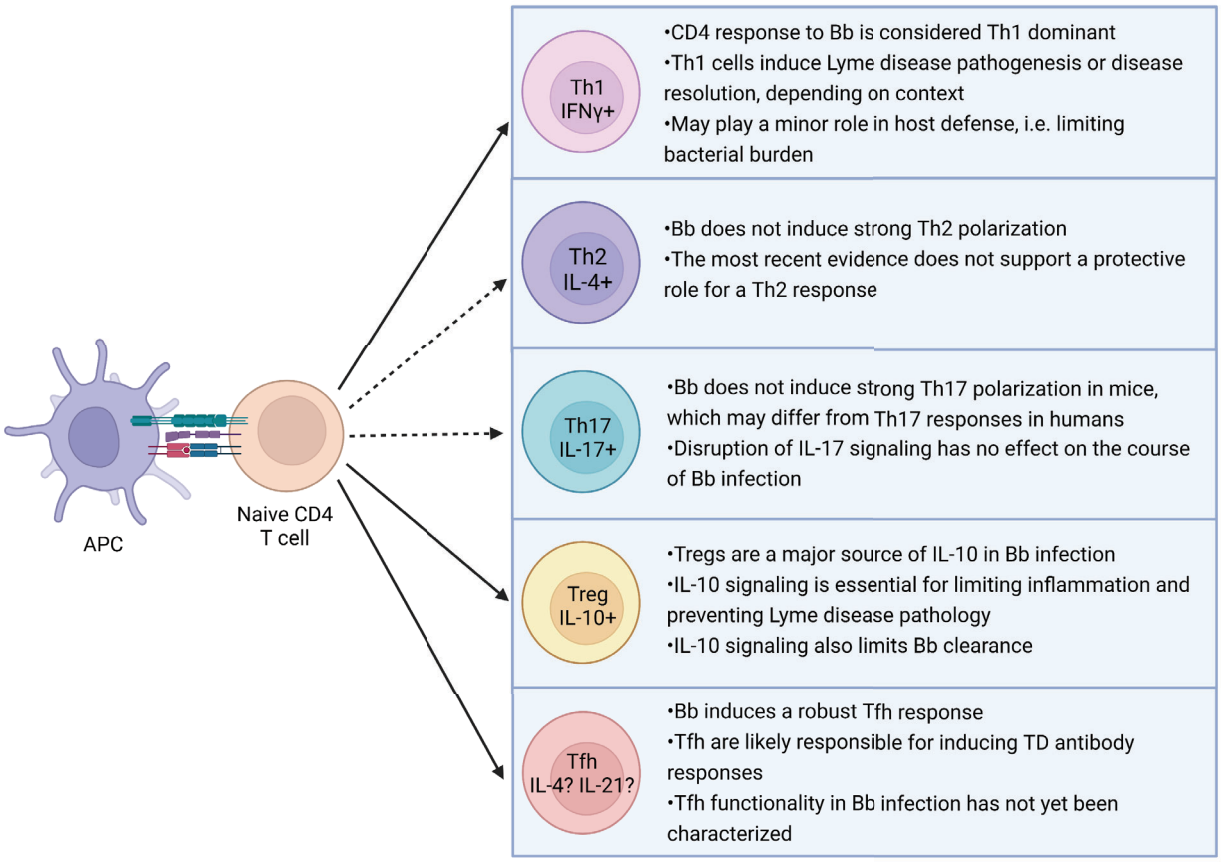

Figure 1.2: Functions of CD4 T cell subsets in Bb infection. Upon priming and activation by antigen presenting cells (APCs), CD4 T cells differentiate into cells expressing a distinct set of co-stimulatory molecules, chemokine receptors and cytokines regulating their migration and function. Shown are five major CD4 T cell subsets (Th1, Th2, Th17, Treg, and Tfh), their key cytokine profile and their known effects on the course of Bb infection in mice.

Chapter 2

Lack of effector CD4 T cell polarization during persistent infection of mice with *Borrelia burgdorferi*

2.1 Abstract

Borrelia burgdorferi (Bb), the spirochetal agent of Lyme disease, evades immune clearance in infected mice, establishing bacterial persistence. To determine host cell targets of Bb immune evasion we examined the functionality of CD4 T cells in Bb infection, which was previously considered to evoke a Th1 dominant immune response. However, since Th1 responses are generally associated with intracellular pathogens, but Bb is an extracelluar bacteria, we decided to reexamine CD4 T cell polarization in Bb infection. Analysis of the polarization state of activated LN and blood effector CD4 T cells throughout Bb infection by quantitative RT-PCR and flow cytometry revealed the presence of only modest numbers of Th1-polarized activated CD4 T cells, as measured by expression of Tbet (*Tbx21*), and little to no induction of *Ifng*. In contrast, Tfh (Bcl6+CXCR5+ $PD1^{hi}$) differentiation was induced strongly during early infection, but these Tfh cells disappeared with the collapse of germinal centers around one month after infection. The lack of effector CD4 Th1 polarization was not explained by strongly enhanced polarization towards FoxP3+ CD4 Treg, or Th2 and Th17 polarization, as GATA-3 and RORγt expression were also largely absent from the activated CD4 T cell pool. Nor was it explained by polarization at an effector site, as skin-resident CD4 T cells also showed no evidence of polarization, even five months after infection. Together, our data demonstrate a lack of CD4 T cell polarization during Bb infection, and suggest a dysregulation of effector CD4 T cell responses during persistent Bb infection.

2.2 Introduction

CD4 T helper cells play an essential role in coordinating inflammatory responses as part of the host defense against pathogens. As CD4 T cells undergo activation by antigen presenting cells (APCs), they receive instructions to undergo polarization that is appropriate and effective to the type of microbe that is currently invading the host environment [1-3]. Inappropriate T cell polarization has been implicated in enhanced pathology as well as failure to eradicate infection [4,5].

Multiple types of CD4 T cell polarization have been identified and linked to specialized functions. Briefly, Th1 polarization is typically seen in response to intracellular pathogens, such as viruses and intracellular bacteria; Th2 polarization is generally induced by parasitic helminths; and Th17 responses are induced by infections with yeast as well as extracellular bacterial pathogens [6-8]. In addition to these effector subsets, CD4 T cells can also polarize to a T follicular helper (Tfh) phenotype, which are programmed to migrate to the B cell follicle of lymphoid tissues and provide specialized support to antigen (Ag)-experienced B cells [9-11]. Lastly, anti-inflammatory regulatory T cells (Treg) can become polarized either during thymic development or in the periphery [12].

CD4 T cell polarization is controlled at the transcriptional level by induction of lineage-defining transcription factors (TFs). These TFs include Tbet, GATA3, RORγt, Bcl6, and Foxp3 that mediate differentiation of Th1, Th2, Th17, Tfh, and Treg phenotypes, respectively [13]. These TFs promote cytokine production specific to each T helper subtype [14]. However, individual CD4 T cells display differing degrees of plasticity, including the ability to express multiple lineage-specific TFs and cytokines at once, as well as the ability to modulate subtype identity completely [15,16]. Although the reality of CD4 T cell polarization is more complex than this simple paradigm of five T helper lineages suggests [17], it is nonetheless a useful tool for understanding the role of CD4 T cell effector functions in many different contexts.

In the course of *Borrelia burgdorferi* (Bb) infection, effector CD4 T cells are thought to predominantly undergo Th1 polarization, even though Bb largely reside in the extracellular environment of the host. Although studies have found that T cells are largely dispensable in controlling Bb infection [18,19], Th1 cells have been shown to play a minor role in controlling Bb burden and in resolving Lyme carditis [20,21]. Otherwise, most studies have focused on the role of IFNγ-secreting T cells in causing Lyme pathology [22-24]. The poorly protective, and potentially pathogenic, nature of a Th1 dominant CD4 T cell response to Bb infection calls into question whether Th1 polarization is an effective or appropriate defense against Bb.

More recent studies have investigated whether Th17 polarized T cells play a role in Bb infection. One study found little evidence for induction of IL-17 secreting cells by Bb, although the Th17 cytokine IL-22 was induced [25]. Another group has shown that IL-17 was associated with enhanced Lyme arthritis in a mouse model using heterologous Bb priming prior to infection [26,27]. However, Lasky et al. found that deletion of IL-17RA had no effect on the course of disease in a model of primary Bb infection, indicating a limited role for Th17 polarization [28].

Our lab previously examined the formation of Tfh in Bb infection, and observed strong Tfh induction coinciding with germinal center (GC) formation [29]. Despite robust Tfh cell induction, GCs are not sustained and disappear approximately 28 days post infection (dpi) with Bb. We observed neither upregulation of T cell exhaustion markers on Tfh, nor evidence of aberrant regulatory Tfh (Tfr) induction, to explain why Tfh fail to sustain GCs [30]. Instead, we found that Bb infection altered the nature of T cell-B cell interactions, favoring Ab production over B cell proliferation [30].

The role of immunosuppressive Treg in modulating Bb pathology is also of keen interest, since insufficient immune regulation can cause pathology, whereas too much immune suppression may contribute to bacterial persistence. Indeed, Brown et al. showed that genetic deletion of the major Treg cytokine IL-10 led to enhanced control of Bb numbers, albeit at the expense of increased arthritis of the large joints [31]. Subsequent characterization of the IL-$10^{-/-}$ model of Lyme arthritis confirmed that increased arthritis severity was likely mediated by CD4 T cells, as well as macrophages [32]. Similarly, Vudattu et al. demonstrated a correlation between decreased Treg in the synovial fluid of treatment refractory Lyme arthritis patients and prolonged arthritis symptoms [33].

Despite the wealth of literature devoted to revealing the role of different T helper subsets in the pathogenesis of Lyme disease, the extent to which each CD4 subtype contributes to the overall immune response in Bb infection is still unclear. Here, we provide a comprehensive study of CD4 T cell polarization in a mouse model of Bb infection, including characterization at an important T cell effector site, the skin. Unexpectedly, we observed an overall dearth of polarized effector CD4 T cells (Teff) in lymphoid and effector tissues with only a small frequency of Tbet+ Th1 polarized T cells both at early and late timepoints after Bb infection. Together the data suggest that dysregulated Teff responses might contribute to the ability of Bb to establish persistence in an immunocompetent host.

2.3 Results

To assess the functionality of CD4 Teff during Bb infection we first aimed to characterize CD4 T cell activation in the draining inguinal LN of mice, which we infected with host-adapted spirochetes in the right lower hind leg, measuring CD4 T cell numbers at various intervals using flow cytometry in the draining inguinal lymph node (LN). As we observed previously [29,34], there was a very strong increase in the LN cellularity after Bb infection. However, expansion of total CD4 T cells in the LN was only

modest, particularly when compared to the increases in total B cell numbers (**Fig. 2.1A, B**). At the height of LN cellularity (10 dpi), B cell numbers had increased more than 16-fold compared to 0 dpi, while CD4 T cells increased about 5.5-fold (**Fig. 2.1B**). By the time of the germinal center collapse in the LN, which we had described previously to occur around day 28 dpi [29,35], B cells still outnumbered CD4 T cells by more than 3:1, compared to a ratio of 1.5:1 before infection. In contrast to the large proportion of naïve B cells recruited to the draining LN after Bb infection [29], the number of $CD44^{hi}$ $CD11a^{hi}$ activated CD4 T cells increased over 20-fold by 14 dpi (**Fig. 2.1C, D**).

We noticed a reproducible, temporary decrease in activated CD4 T cells at 19 dpi in the draining LN, followed by a rebound by 22 dpi. Because this could be due to egress of activated CD4 T cells from the LN to sites of inflammation, we also analyzed CD4 T cells in the peripheral blood and the spleen. Correlating with the drop in activated LN CD4 T cells at 19 dpi, CD4 T cells were significantly increased in in the peripheral blood, as well as spleen at 20 dpi (**Fig. 2.1E**). Together, the data show that CD4 T cells undergo dynamic activation and migration throughout Bb infection.

Early CD4 T cell differentiation after Bb infection is dominated by Bcl6-expressing cells

Next, we assessed CD4 T cell differentiation by measuring expression of master transcription factors (TF) and cytokines associated with various T helper lineages (Th1, Th2, Th17, Tfh, and Treg), using quantitative RT-PCR on magnetically enriched CD4 T cells from LNs of mice at days 8 and 14 dpi. To account for inflammation contributed by the mode of infection (subcutaneous tissue transplant), we included a sham infection control group which was analyzed at 8 dpi. In agreement with previous studies that had described the CD4 T cell response as Th1 dominant, *Tbx21* expression was increased more than 6-fold at 8 dpi compared to naïve controls (**Fig. 2.2A**). However, *Tbx21* induction was transient. By 14 dpi *Tbx21* expression was not significantly different than that of non-infected mice ($p=0.7087$, one-way

ANOVA with Tukey's post-hoc comparison). Surprisingly, transcript levels of the Th1 cytokine IFNγ were not significantly increased over naïve levels at either 8 or 14 dpi (**Fig. 2.2B**, p=0.488). The TFs *Gata3* and *Rorc* and cytokines *Il4*, and *Il17*, which are associated with Th2 and Th17 differentiation, respectively, and can act as antagonists to Th1 polarization; these were not significantly increased in Bb infected groups. A minor exception was a transient and highly variable increase of *Il17a* at 8 dpi (**Fig. 2.2B**).

Th1 cells have previously been associated with Lyme pathogenesis [22,36] and B6 mice are resistant to many aspects of Bb induced pathology [37,38]. We therefore also tested whether genetic susceptibility to Lyme arthritis affected T helper polarization by measuring CD4 T cell polarization in B6-congenic *Gusb*^{h} mice (breeders provided by Janis Weis, University of Utah), which develop Lyme arthritis due to lack of β-glucoronidase and a resulting failure to remove DAMPS from the infected joints [39]. However, in this model also, CD4 effector cytokines and transcriptional regulators were comparable in *Gusb*^{h} and B6 mice on days 8 and 14 of infection (**Fig. 2.2A, B**).

We also observed a modest (1.6-fold) increase in *Foxp3* expression in Bb infected mice at 8 but no significant change at 14 dpi (**Fig. 2.2A**). Significant increases in *Il10* expression were noted in the GusB mice at 8 dpi compared to either non-infected (D0) or sham-infected B6 mice (D8). Although we also noted modest increases in *Il10* expression in infected B6 mice (D8 and D14), those increases did not reach statistical significance (p=0.1243 B6 D0 vs. B6 D8; p=0.3808 B6 D0 vs. B6 D14). Thus, IL-10 appeared at best only modestly induced in the lymph node CD4 T cells at these early time points after Bb infection. In contrast to the modest induction of TF that drive Teff polarization, we observed a robust induction of the regulator of Tfh development, *Bcl6 (3-fold),* and the corresponding signature cytokine, *Il21 (>80-fold;* **Fig. 2.2A, B**). We conclude that within 1-2 weeks following Bb infection CD4 T cells in

the LN strongly polarized towards a Tfh phenotype, while evidence of effector CD4 T cell differentiation was largely absent at that site.

Strong Tfh but not effector CD4 T cell differentiation after Bb infection

We next analyzed CD4 polarization at the single cell level in LN of mice at 10 and 14 dpi using flow cytometry. In addition to lineage markers, cells were stained simultaneously for Tbet, GATA3, RORγt, Foxp3, and Bcl6. To distinguish expression of these TF in naïve and activated CD4 T cells we also stained for CD44 and CD11a (**Fig. 2.3A, left panel**). To identify appropriate gates to distinguish TF+ from TF- cells, "Fluorescence minus one" (FMO) controls (**Fig. 2.3A** bottom panels), and when available staining of gene-targeted mice (**Fig. 2.4A-C**), were used. Successful staining for TF expression was confirmed on thymocytes (**Fig. 2.4A-C**). TF expression analysis of $CD11a^{lo}$ $CD44^{int}$ CD4 T cells confirmed the low abundance of all TFs in naïve T cells, with the exception of FoxP3, as expected (**Fig. 2.3A,** middle panels). As expected also, the most common TF in the small number of activated, $CD11a^{hi}$ $CD44^{hi}$ CD4 T cells present in LN, spleen and PBMC of non-infected mice was Foxp3 (**Fig. 2.3B**), indicating the presence of Tregs, which play an essential role in maintaining immune homeostasis[12]. A portion of Foxp3 expressing cells also co-expressed GATA3, which is important for Treg function and maintenance[40].

Following Bb infection, >50% of TF+ activated CD4 T cells in the draining LN co-expressed multiple transcription factors at 10 dpi (**Fig. 2.3B**). By 14 dpi, a clearer pattern of CD4 T cell polarization began to emerge (**Fig. 2.3A top panel, B**). Consistent with the qRT-PCR analysis, Bcl6+ Tfh-like cells were the dominant TF+ population in the draining LN, as well as the TF+ population with the greatest number of single TF expressing cells (**Fig. 2.3A, B**). Among circulating PBMC, Tbet+ Th1-like activated CD4 T cells were more prevalent than GATA3+ or Foxp3+ cells. Even so, only half of Tbet+ activated CD4 T

cells in PBMCs did not express additional TFs. In spleen, Foxp3+ Tregs outnumbered all other TF+ cells (**Fig. 2.3B**), consistent with our previous observations that the spleen is not a major site of immune induction in this Bb infection model [34]. The proportion of TF negative but activated CD4 T cells remained similar in the draining LN before and after infection, but increased in spleen and among PBMCs. We designated the population of TF negative cells as Th0/other, since these cells could have undergone a type of polarization not assayed here. The analysis confirmed and expanded the results of the qRT-PCR analysis, demonstrating a notable polarization of CD4 T cells in the LN towards single Bcl6-expressing Tfh, but an at best modest induction of activated CD4 Teff, with nearly all such cells co-expressing multiple TFs.

Since we observed the largest proportion of single TF+, CD4 Th1 (Tbet+) cells among PBMCs, we considered that CD4 Teff might polarize only following their migration from the site of activation in the draining LN to an effector site. We focused on the skin, an important reservoir for Bb[41] and the site of bacterial transfer to and from ticks. Although sufficient numbers of activated CD4 T cells were not present in skin of non-infected mice to conduct TF analysis, by 14 dpi, >1,000 CD4 T cells per mouse skin digest (roughly 11% of total skin leukocytes) had accumulated, of which most expressed an activated $CD44^{hi}$ $CD11a^{hi}$ phenotype (**Fig. 2.5A**). Unexpectedly, nearly 70% of these activated CD4 cells from skin failed to express any of the assayed TFs at 14 dpi. Although Tbet+ cells were found in greater numbers than other effector types, approximately half of the Tbet+ cells co-expressed additional TFs, and the total Tbet+ cells contributed only 13% to the overall activated CD4 T cell pool (**Fig. 2.5A**). This lack of T cell polarization was not due to contamination of the skin cell preparation with T cells from the capillary bed, as intravenous injection of an anti-CD45.2 mAb [42] to stain intravenous leukocytes 3 minutes before necropsy showed that only about 6% of CD4 T cells were stained and thus likely blood-derived at necropsy (**Fig. 2.5B**).

In summary, strong CD4 Teff polarization is absent during the first two weeks post infection with Bb in secondary lymphoid tissues, PBMC and the skin, the latter an important effector site. Indeed, CD4 T cell polarization appeared weakest at the effector site, despite the fact that the majority of skin CD4 T cells were activated (**Fig. 2.5A**).

Lack of CD4 T cell polarization during persistent Bb infection

We considered whether CD4 T cell polarization might increase over time in persistently infected animals and conducted similar flow cytometric evaluation of CD4 Teff at 30 and 160 dpi. The data were consistent with those obtained at early time points, demonstrating that only a few polarized Teff were present in any of the tissues analyzed, including the LN, skin (**Fig. 2.6),** PBMC and spleen (**Fig. 2.7**). In the LN, there was a significant decrease in Bcl6+ cells beginning at 30 dpi compared to 14 dpi (**Fig. 2.6A**), temporally coinciding with the collapse of germinal centers [29,35] . The proportion of Bcl6+ cells in the draining LN did not recover between 30 and 160 dpi, and the total CD4 T cells numbers in the LN strongly contracted over this time (**Fig. 2.6C**). Bcl6+ Tfh made up approximately 20% of all activated CD4 T cells in both persistently infected and age-matched naïve animals (**Fig. 2.6A**).

The proportion, but not absolute number, of Foxp3+ Tregs increased over time in the draining LN of persistently infected mice (**Fig. 2.6A, C**), although this was independent of infection, since naïve age-matched mice had a similar proportion of Foxp3+ cells (39%) compared to mice infected for 160 days (34%, p=0.4333). In PBMC, frequencies of Foxp3+ Tregs increased transiently at 30 dpi, and then, in persistent infection, returned to levels similar to those seen at 14 dpi (**Fig. 2.7A**). There was no significant difference in the frequency of Foxp3+ CD4 T cells over the course of infection in skin or spleen (**Figs. 2.6B and 2.7B)**.

Interestingly, the frequencies of TF+ CD4 T cells were not different between infected mice at 160 dpi and naïve age-matched controls, although the number of skin resident CD4 T cells was significantly higher in infected mice compared to naïve mice (**Fig. 2.6B, D**). Thus, CD4 T cells accumulate in the skin over the course of Bb infection, but effector polarization does not increase over time. We conclude that robust CD4 Teff polarization did not occur in mice persistently infected with Bb.

2.4 Discussion

CD4 T cell responses, through their production of cytokines, are critical for the regulation of adaptive immunity to many infections. The nature and effectiveness of the T cell help depends on appropriate polarization of uncommitted naïve CD4 T cells to polarization into effector T cells that produce critical cytokines to guide the immune response. By conducting a thorough characterization of CD4 T cell responses to Bb infection in persistently infected mice, we demonstrated significant CD4 T cell activation and expansion at the site of immune induction (the draining LN), as well as accumulation at an important effector site (the skin). Surprisingly, however, we noted a lack of vigorous Teff polarization (Th1, Th2, or Th17) of CD4 T cells at either site, at both early and late phases of this persistent infection.

Of the T effector polarization states that we analyzed, our data show that more Tbet+ Th1 cells were induced following Bb infection compared to Th2 or Th17 polarized cells, consistent with previous studies that demonstrated a Th1 dominant response to Bb [32,36,43,44]. Unexpectedly, our data revealed relatively weak Th1 polarization as measured by the percent of activated CD4 that expressed Tbet, as well as a lack of IFNγ induction. This could be explained, in part, by our use of C57BL/6 mice, which are reported to produce lower levels of IFNγ in response to Bb than other strains [37]. However, in other studies that had assessed IFNγ induction directly *ex vivo,* rather than by re-stimulation, also showed weak IFNγ induction in both Lyme disease-susceptible (C3H) and -resistant (C57BL/6) mouse strains [45,46].

Our data suggest that in response to Bb infection, CD4 T cells are primed to undergo Th1 polarization, but are not fully differentiated into effector cells that produce the canonical Th1 proinflammatory cytokine IFNγ.

Although we were able to find a small number of RORγt expressing CD4 T cells in Bb infected mice, we did not observe evidence of significant Th17 polarization. This is consistent with a Th1 dominant response, since Tbet directly inhibits Th17 polarization [47]. Furthermore, the observed lack of Th17 polarization may help explain why Bb infected mice deficient in IL-17 signaling molecules did not show enhanced bacterial tissue loads [28,48].

In contrast to the weak polarization we observed in effector CD4 subsets, we observed strong Tfh polarization in the draining LN at 14 dpi. Tfh numbers were much lower at 30 dpi, consistent with both the timing of the GC collapse [29], as well as the similar observations by others [29,49]. Although we have previously described strong induction of Tfh [30], this observation contrasts with the failure to maintain the GC reaction during Bb infection. Since our qRT-PCR analysis showed a strong increase in *Il21* transcripts following Bb infection, it appears that the Tfh fulfill this critical Tfh effector function. Nonetheless, further studies are warranted to test the functionality of Tfh induced by Bb infection.

The final CD4 subset of note were Foxp3+ Tregs. By late infection, Tregs represented the largest population of CD4+ TF+ cells in both the draining LN and the skin. However, the proportion of Foxp3+ CD4 T cells was not different in late infection compared to age-matched naïve controls. Additionally, we observed only modest CD4-specific expression of IL-10. These results argue against an overly abundant Treg response to Bb infection, and instead support the role of Tregs in limiting Bb induced pathology [32].

To our knowledge, our study represents the first attempt to characterize the polarization of the CD4 response to Bb in the skin. Surprisingly, of all the tissues we analyzed, skin resident CD4 T cells had the weakest overall CD4 polarization (i.e. skin had the highest percent of Th0/other CD4 T cells). Because skin resident CD4 T cells were largely unpolarized, these cells were not likely secreting lineage specific effector cytokines, such as IFNγ. Given that CD4 T cells play an essential role in orchestrating inflammation in infected tissues, as well as activating macrophages and granulocytes, our data raise the possibility that Bb inhibits strong CD4 T cell polarization as a means of evading immune-mediated clearance, supporting the establishment of persistence in the skin of infected hosts.

Because our expression analysis was restricted to the TFs and cytokines associated with five canonical CD4 T cell subsets (Th1, Th2, Th17, Tfh, and Treg), we cannot exclude the possibility that another type of CD4 T cell polarization is induced in our model of Bb infection. Expression analysis of additional cytokines and markers of known CD4 T cell subsets (such as Th9, Th22, and Tr1) is warranted to further elucidate CD4 T cell polarization in Bb infection. However, other Bb studies that use less biased methods of immune cell expression profiling, such as RNA-seq, have not provided evidence that would point toward strong induction of any known alternative CD4 T helper subset [50].

Although we have characterized CD4 T cell activation and polarization with these studies, we have not addressed whether CD4 T cells are able to respond to Bb infection in an Ag-specific manner. Others have demonstrated that Bb can induce non-specific bystander T cell activation [51], but there are currently no reagents or mouse models available to evaluate Ag specific T cell responses in a mouse model of Bb infection. In order to understand mechanisms by which Bb is able to evade the CD4 T cell response, there is an urgent need to develop tools to characterize Ag-specific T cell responses.

Furthermore, our data do not address the functional role of differentially polarized CD4 T cells in Bb infection. Although CD4 T cells have been implicated in providing protection against Bb replication and dissemination [30], the role of different CD4 subsets is less clear. Future studies on the role of CD4 T cell polarization may provide insights into the optimal balance of CD4 T cell polarization that can promote control and clearance of spirochetes, while minimizing tissue pathology.

Here we provide a thorough characterization of CD4 T cell polarization in Bb infected mice in the absence of genetic or pharmacologic manipulation. These data provide a useful framework for understanding host-pathogen interactions between mice and Bb, and help contextualize some of the existing studies that examine the CD4 response to Bb infection. Additionally, our data suggest that Bb inhibits strong effector CD4 T cell polarization as a means of evading immune clearance, providing a novel potential therapeutic target.

2.5 Materials and Methods

Mice

Unless otherwise noted, mice were purchased from Jackson laboratory. Strains include C57BL/6 (000664), B6.Cg-*Prkdc*^{scid}/SzJ (B6-SCID, 001913), and B6.129S6-*Tbx21*^{tm1Glm}/J (004648). Mice were housed in microisolator cages under specific pathogen free conditions. Females at 8 to 12 weeks of age were used for all experiments unless otherwise specified. Prior to tissue harvesting, mice were euthanized by overexposure to CO_2. All procedures were performed with approval from the University of California, Davis Animal Care and Use Committee.

Borrelia burgdorferi infections

A low passage clonal strain of *Borrelia burgdorferi sensu stricto* (cN40) was grown in modified Barbour-Stoenner-Kelley (BSK) II medium as previously described [29,34]. *B. burgdorferi* were grown to mid-log phase and enumerated using a Petroff–Hauser bacterial counting chamber. B6-SCID mice were injected subcutaneously (s.c.) with 10^4 spirochetes diluted in BSK. After 2-6 weeks of infection, ear pinnae were harvested from infected SCID mice, cleaned with Novalsan (Zoetis) and 70% ethanol, and trimmed into 8 sections. Ear pieces were transplanted s.c. at the right rear hock of experimental mice using a stab incision. Prior to transplant, experimental mice were placed under anesthesia with a mixture of ketamine (10 mg/kg) and xylazine (1 mg/kg). Anesthetized mice also received an NSAID analgesic (either 7.5 mg/kg meloxicam or 5 mg/kg carprofen), and incision site was monitored for 7 days after surgery. For sham infections, naïve SCID ear tissue was transplanted into right rear hock of C57BL/6 mice, as described above.

Flow Cytometry

Single cell suspensions of inguinal LNs, spleen, and thymus were prepared for flow cytometric analysis as described previously [29,30]. Briefly, tissues were ground between glass slides, and treated with ammonium chloride potassium (ACK) lysis buffer if erythrocyte contamination was evident. After filtering single cell suspensions over a 70 μm nylon mesh filter and enumerating via hemocytometer, cells were Fc blocked using in house generated anti-CD16/CD32 (clone 2.4G2). Cells were then stained with combinations of the following antibodies (*conjugate clone manufacturer*): CD3 (Alexa700 500A2 Invitrogen, PerCP-ef710 17A2 Invitrogen), CD4 (APC-ef780 GK1.5 Invitrogen, Alexa700 RM4-5 Invitrogen, Cy7-PE GK1.5 in house), CD19 (BV786 ID3 BD Biosciences, PE-CF594 ID3 Invitrogen, Biotin ID3 in house), B220 (APC-ef780 RA3-6B2 Invitrogen), CD44 (BV711 IM7 Biolegend), CD11a (PE M17/4 Invitrogen, Cy7-PE 2D7 BD Biosciences), CD62L (BV605 MEL-14 BD Biosciences), ICOS (BUV395 C398.4A BD Biosciences, FITC in house), PD-1 (BV421 J43 BD Biosciences), CXCR5 (BV785 L138D7 Biolegend, Biotin 2G8 BD Biosciences), CD8a (Alexa700 53-6.7 Invitrogen, PE and

Biotin 53.6.7.3.1 in house), NK1.1 (Alexa700 PK136 Invitrogen, Biotin PK136 Biolegend), Gr-1 (red fluor 710 1A8 Tonbo, Biotin RA3.6C2 in house), F4/80 (Cy5-PE BM8 Biolegend, Alexa700 BM8 Biolegend, Biotin F4/80 in house), TCR γ/δ (Biotin GL3 in house), CD45 (BUV395 30-F11 BD Biosciences), Ly6C (BV785 HK1.4 Biolegend), Streptavidin (BV605 Cat# 405229 Biolegend, APC Cat# 17-4317-82 Invitrogen), Bcl6 (Alexa647 K112-91 BD Biosciences), Foxp3 (FITC FJK-16s Invitrogen), GATA3 (PerCP-ef710 TWAJ Invitrogen), RORγt (PE-CF594 Q31-378 BD Biosciences), Tbet (Cy7-PE 4B10 Invitrogen). Extracellular labeling was performed on ice for 20 minutes. For intracellular labeling, cells were fixed and permeabilized with Foxp3 Transcription Factor Staining Buffer Set (eBioscience 00-5523-00) following manufacturer's instructions. Intracellular antibodies were incubated for 30 minutes at room temperature. Data was acquired on either a LSRFortessa or FACSymphony flow cytometer (BD), and analyzed using FlowJo software.

PBMC processing for FACS

Whole blood was collected by cardiac puncture into lithium heparin coated microtainer tubes (BD Biosciences 365965). Blood volume was measured and diluted in 4-5 mL KDS-BSS prior to overlaying on top of 6 mL room temperature Ficoll Paque Plus (GE). PBMCs were separated by centrifugation at 700 x*g* for 20 minutes with no brake, at room temperature. When erythrocyte contamination was visible, samples were treated with ACK lysis buffer for 1-2 minutes prior to filtration over a 70 μm nylon filter and enumeration via hemocytometer. Cell labeling and analysis were as described above (Flow Cytometry).

Intravenous labeling of circulating leukocytes

Anti-CD45.2 (104 FITC Invitrogen) was diluted in sterile PBS at 15 µg/mL. 200 µL per mouse was injected into tail vein 3 minutes prior to euthanasia by CO_2 overexposure [42]. Tissues were prepared and labeled for flow cytometry analysis as described above.

Magnetic Separation of CD4 T cells

The draining (right inguinal) LN was harvested and processed as above (Flow cytometry), and labeled with biotinylated Abs and anti-biotin microbeads (Miltenyi 130-090-485). Total CD4 T cells were enriched by magnetic separation of non-T cell populations (CD19+, CD8a+, Gr-1+, F4/80+, NK1.1+, TCR γ/δ+) via AutoMACS Pro Separator (Miltenyi Biotec). An aliquot from the negative fraction was labeled with Streptavidin, CD3e, and CD4 antibodies prior to FACS analysis for purity check. CD4 T cell purity of >90% was confirmed for each sample used in downstream analysis. Purity was calculated as percent cells that were CD3e+ CD4+ Streptavidin- of total cells gated on Lymphocytes/Singlets/Live (mean purity was 97.9% ± 1.2% SD).

Relative expression of CD4 T cell genes

CD4 T cells were lysed and RNA from lymphocytes was extracted using Norgen Total RNA Purification Kit (Norgen 17200), following manufacturer's instructions. cDNA was prepared with Superscript II Reverse Transcriptase Kit (Invitrogen 18064014) using random hexameric primers. RT-PCR reaction utilized TaqMan primer/probes and TaqMan Universal PCR Master Mix (Applied Biosystems 4364338). 96 well plates were run using QuantStudios 6 Flex System (Applied Biosystems). All expression values were calculated relative to Ubiquitin C housekeeping gene.

Calculation of % TF+ CD4 T cell pie charts

For pie charts, cells were gated on lymphocytes, singlets, live, CD3+ CD4+, CD44^{hi} CD11a^{hi} (**Fig. 3**). Inner circle represents the mean percent of CD44^{hi} CD11a^{hi} subpopulations (i.e. activated CD4; N=4 animals at each timepoint), either TF+ cells (Bcl6+, Foxp3+, GATA3+, RORγt+, or Tbet+) or TF- cells (i.e. Th0/other, defined as Bcl6- Foxp3- GATA3- RORγt- Tbet-), as determined by gating in FlowJo (**Fig. 3B**). Because some TF+ cells were positive for more than one TF, the sum of all activated CD4 subpopulations was greater than 100%. The sum of means of TF+ plus TF- populations was calculated as:

$$\overline{\%\text{Bcl6}} + \overline{\%\text{Foxp3}} + \overline{\%\text{GATA3}} + \overline{\%\text{RORγt}} + \overline{\%\text{Tbet}} + \overline{\%\text{Th0/other}} = \text{sum value} > 100$$

These values make up the inner circle of each pie chart.

To facilitate analysis, population percentage was normalized to a total of 100%. For that the mean value (X) of TF+ activated CD4 T cells from dLN (%) was divided by the sum % value of TF+ and TF- populations of activated CD4 (Y) then multiplied by 100%:

$$\left(\frac{X\ \%}{Y\ \%}\right) \times 100\% = Normalized\ TF\ (\%)$$

TF+ populations were further analyzed for the expression of multiple TFs, illustrated with an outer ring of the pie charts (**Fig. 3B**). For each TF+ activated CD4 T cell, the mean % TF+ of all other TF was determined, and mean values of multi-TF+ populations (Bcl6+ Foxp3+, Bcl6+ GATA3+, Bcl6+ RORγt+, Bcl6+ Tbet+) or single TF+ populations (Bcl6+ Foxp3- GATA3- RORγt- Tbet-) were determined as percent of activated CD4 T cells. Again, population values were normalized to a total of 100% of activated CD4 T cells. Thus, the normalized value of a particular TF+ cell expressing a second TF was calculated as:

$$\left(\frac{Mean\ \%\ two\ TF+}{Mean\ sum\ total\ TF+}\right) \times 100\% = TF\ coexpression\ (\%)$$

Finally, each multi-TF+ and single-TF+ population was calculated as a proportion of all activated cells by multiplying the population percentage by the percent of the TF+ population in the inner circle.

Skin Digest

Mouse skin was weighed prior to digest. Skin was digested in two 30 minute incubations at 37 C in HBSS with 25 µg/ml Liberase (Roche 5401119001) and 100 µg/ml DNase I (Roche 10104159001). Cells were passed over a 100 µm filter, and immune cells were enriched by 33% Percoll gradient, centrifuged at 600 x*g* for 20 minutes at room temperature [52].

Statistics

All statistics were performed and plots generated using Prism GraphPad software.Statistical tests include one-way ANOVA or 2-way ANOVA, with Tukey's post-hoc comparison, as indicated. P-values were considered significant if $p<0.05$.

Acknowledgements

The authors would like to thank Gudrun Debes for sharing protocols for skin digestion and leukocyte retrieval. Funding was provided by the Global Lyme Alliance and the Alexandra and Steve Cohen Foundation as well as the Center for Immunology and Infectious Diseases, UC Davis.

2.6 References

1. Ross PJ, Sutton CE, Higgins S, Allen AC, Walsh K, Misiak A, Lavelle EC, McLoughlin RM, Mills KHG: **Relative Contribution of Th1 and Th17 Cells in Adaptive Immunity to Bordetella pertussis: Towards the Rational Design of an Improved Acellular Pertussis Vaccine**. *PLOS Pathogens* 2013, **9**:e1003264.
2. Jeitziner SM, Walton SM, Torti N, Oxenius A: **Adoptive transfer of cytomegalovirus-specific effector CD4+ T cells provides antiviral protection from murine CMV infection**. *European Journal of Immunology* 2013, **43**:2886-2895.
3. Xu H, Wang X, Veazey RS: **Mucosal immunology of HIV infection**. *Immunological Reviews* 2013, **254**:10-33.
4. Sato F, Kawai E, Martinez NE, Omura S, Park A-M, Takahashi S, Yoh K, Tsunoda I: **T-bet, but not Gata3, overexpression is detrimental in a neurotropic viral infection**. *Scientific Reports* 2017, **7**:10496.
5. Li M-M, Zhang W-J, Weng X-F, Li M-Y, Liu J, Xiong Y, Xiong S-E, Zou C-C, Wang H, Lu M-j, et al.: **CD4 T cell loss and Th2 and Th17 bias are associated with the severity of severe fever with thrombocytopenia syndrome (SFTS)**. *Clinical Immunology* 2018, **195**:8-17.
6. Butcher MJ, Zhu J: **Recent advances in understanding the Th1/Th2 effector choice**. *Fac Rev* 2021, **10**:30.
7. Curtis MM, Way SS: **Interleukin-17 in host defence against bacterial, mycobacterial and fungal pathogens**. *Immunology* 2009, **126**:177-185.
8. Liu JZ, Pezeshki M, Raffatellu M: **Th17 cytokines and host-pathogen interactions at the mucosa: dichotomies of help and harm**. *Cytokine* 2009, **48**:156-160.
9. Kroenke MA, Eto D, Locci M, Cho M, Davidson T, Haddad EK, Crotty S: **Bcl6 and Maf Cooperate To Instruct Human Follicular Helper CD4 T Cell Differentiation**. *The Journal of Immunology* 2012, **188**:3734-3744.
10. Barnett LG, Simkins HMA, Barnett BE, Korn LL, Johnson AL, Wherry EJ, Wu GF, Laufer TM: **B Cell Antigen Presentation in the Initiation of Follicular Helper T Cell and Germinal Center Differentiation**. *The Journal of Immunology* 2014, **192**:3607-3617.
11. Butler NS, Kulu DI: **The regulation of T follicular helper responses during infection**. *Current Opinion in Immunology* 2015, **34**:68-74.
12. Shevyrev D, Tereshchenko V: **Treg Heterogeneity, Function, and Homeostasis**. *Frontiers in Immunology* 2020, **10**.
13. Zhu X, Zhu J: **CD4 T Helper Cell Subsets and Related Human Immunological Disorders**. *International Journal of Molecular Sciences* 2020, **21**:8011.
14. Li P, Spolski R, Liao W, Leonard WJ: **Complex interactions of transcription factors in mediating cytokine biology in T cells**. *Immunological Reviews* 2014, **261**:141-156.
15. Nakayamada S, Takahashi H, Kanno Y, O'Shea JJ: **Helper T cell diversity and plasticity**. *Current Opinion in Immunology* 2012, **24**:297-302.
16. Geginat J, Paroni M, Maglie S, Alfen JS, Kastirr I, Gruarin P, De Simone M, Pagani M, Abrignani S: **Plasticity of human CD4 T cell subsets**. *Front Immunol* 2014, **5**:630.
17. Chatzileontiadou DSM, Sloane H, Nguyen AT, Gras S, Grant EJ: **The Many Faces of CD4+ T Cells: Immunological and Structural Characteristics**. *International Journal of Molecular Sciences* 2021, **22**:73.
18. Fikrig E, Barthold SW, Chen M, Chang CH, Flavell RA: **Protective antibodies develop, and murine Lyme arthritis regresses, in the absence of MHC class II and CD4+ T cells**. *The Journal of Immunology* 1997, **159**:5682-5686.
19. McKisic MD, Barthold SW: **T-cell-independent responses to Borrelia burgdorferi are critical for protective immunity and resolution of lyme disease**. *Infect Immun* 2000, **68**:5190-5197.

20. Anguita J, Persing DH, Rincon M, Barthold SW, Fikrig E: **Effect of anti-interleukin 12 treatment on murine lyme borreliosis**. *The Journal of Clinical Investigation* 1996, **97**:1028-1034.
21. Bockenstedt LK, Kang I, Chang C, Persing D, Hayday A, Barthold SW: **CD4+ T Helper 1 Cells Facilitate Regression of Murine Lyme Carditis**. *Infection and Immunity* 2001, **69**:5264-5269.
22. Matyniak JE, Reiner SL: **T helper phenotype and genetic susceptibility in experimental Lyme disease**. *The Journal of Experimental Medicine* 1995, **181**:1251-1254.
23. Zeidner NS, Dolan MC, Massung R, Piesman J, Fish D: **Coinfection with Borrelia burgdorferi and the agent of human granulocytic ehrlichiosis suppresses IL-2 and IFNγ production and promotes an IL-4 response in C3H/HeJ mice**. *Parasite Immunology* 2000, **22**:581-588.
24. McKisic MD, Redmond WL, Barthold SW: **Cutting Edge: T Cell-Mediated Pathology in Murine Lyme Borreliosis**. *The Journal of Immunology* 2000, **164**:6096-6099.
25. Bachmann M, Horn K, Rudloff I, Goren I, Holdener M, Christen U, Darsow N, Hunfeld K-P, Koehl U, Kind P, et al.: **Early Production of IL-22 but Not IL-17 by Peripheral Blood Mononuclear Cells Exposed to live Borrelia burgdorferi: The Role of Monocytes and Interleukin-1**. *PLOS Pathogens* 2010, **6**:e1001144.
26. Nardelli DT, Luedtke JO, Munson EL, Warner TF, Callister SM, Schell RF: **Significant differences between the Borrelia-infection and Borrelia-vaccination and -infection models of Lyme arthritis in C3H/HeN mice**. *FEMS Immunol Med Microbiol* 2010, **60**:78-89.
27. Hansen ES, Johnson ME, Schell RF, Nardelli DT: **CD4+ cell-derived interleukin-17 in a model of dysregulated, Borrelia-induced arthritis**. *Pathogens and Disease* 2016, **74**:ftw084-ftw084.
28. Lasky CE, Jamison KE, Sidelinger DR, Pratt CL, Zhang G, Brown CR: **Infection of Interleukin 17 Receptor A-Deficient C3H Mice with Borrelia burgdorferi Does Not Affect Their Development of Lyme Arthritis and Carditis**. *Infection and Immunity* 2015, **83**:2882-2888.
29. Hastey CJ, Elsner RA, Barthold SW, Baumgarth N: **Delays and diversions mark the development of B cell responses to Borrelia burgdorferi infection**. *J Immunol* 2012, **188**:5612-5622.
30. Elsner RA, Hastey CJ, Baumgarth N: **CD4+ T cells promote antibody production but not sustained affinity maturation during Borrelia burgdorferi infection**. *Infect Immun* 2015, **83**:48-56.
31. Brown JP, Zachary JF, Teuscher C, Weis JJ, Wooten RM: **Dual Role of Interleukin-10 in Murine Lyme Disease: Regulation of Arthritis Severity and Host Defense**. *Infection and Immunity* 1999, **67**:5142-5150.
32. Sonderegger FL, Ma Y, Maylor-Hagan H, Brewster J, Huang X, Spangrude GJ, Zachary JF, Weis JH, Weis JJ: **Localized Production of IL-10 Suppresses Early Inflammatory Cell Infiltration and Subsequent Development of IFN-γ–Mediated Lyme Arthritis**. *The Journal of Immunology* 2012, **188**:1381-1393.
33. Vudattu NK, Strle K, Steere AC, Drouin EE: **Dysregulation of CD4+CD25high T Cells in the Synovial Fluid of Patients With Antibiotic-Refractory Lyme Arthritis**. *Arthritis & Rheumatism* 2013, **65**:1643-1653.
34. Tunev SS, Hastey CJ, Hodzic E, Feng S, Barthold SW, Baumgarth N: **Lymphoadenopathy during lyme borreliosis is caused by spirochete migration-induced specific B cell activation**. *PLoS Pathog* 2011, **7**:e1002066.
35. Elsner RA, Hastey CJ, Olsen KJ, Baumgarth N: **Suppression of Long-Lived Humoral Immunity Following Borrelia burgdorferi Infection**. *PLoS Pathog* 2015, **11**:e1004976.
36. Gross DM, Steere AC, Huber BT: **T helper 1 response is dominant and localized to the synovial fluid in patients with Lyme arthritis**. *J Immunol* 1998, **160**.
37. Ganapamo F, Dennis VA, Philipp MT: **Differential acquired immune responsiveness to bacterial lipoproteins in Lyme disease-resistant and -susceptible mouse strains**. *European Journal of Immunology* 2003, **33**:1934-1940.
38. Ma Y, Seiler KP, Eichwald EJ, Weis JH, Teuscher C, Weis JJ: **Distinct Characteristics of Resistance to *Borrelia burgdorferi*-Induced Arthritis in C57BL/6N Mice**. *Infection and Immunity* 1998, **66**:161-168.

39. Bramwell KK, Ma Y, Weis JH, Chen X, Zachary JF, Teuscher C, Weis JJ: **Lysosomal β-glucuronidase regulates Lyme and rheumatoid arthritis severity**. *J Clin Invest* 2014, **124**:311-320.
40. Wang Y, Su Maureen A, Wan Yisong Y: **An Essential Role of the Transcription Factor GATA-3 for the Function of Regulatory T Cells**. *Immunity* 2011, **35**:337-348.
41. Hyde JA, Weening EH, Chang M, Trzeciakowski JP, Höök M, Cirillo JD, Skare JT: **Bioluminescent imaging of Borrelia burgdorferi in vivo demonstrates that the fibronectin-binding protein BBK32 is required for optimal infectivity**. *Molecular Microbiology* 2011, **82**:99-113.
42. Anderson KG, Mayer-Barber K, Sung H, Beura L, James BR, Taylor JJ, Qunaj L, Griffith TS, Vezys V, Barber DL, et al.: **Intravascular staining for discrimination of vascular and tissue leukocytes**. *Nature protocols* 2014, **9**:209-222.
43. Hedrick MN, Olson CM, Jr., Conze DB, Bates TC, Rincon M, Anguita J: **Control of Borrelia burgdorferi-specific CD4+-T-cell effector function by interleukin-12- and T-cell receptor-induced p38 mitogen-activated protein kinase activity**. *Infect Immun* 2006, **74**:5713-5717.
44. Yssel H, Shanafelt MC, Soderberg C, Schneider PV, Anzola J, Peltz G: **Borrelia burgdorferi activates a T helper type 1-like T cell subset in Lyme arthritis**. *The Journal of Experimental Medicine* 1991, **174**:593-601.
45. Crandall H, Dunn DM, Ma Y, Wooten RM, Zachary JF, Weis JH, Weiss RB, Weis JJ: **Gene expression profiling reveals unique pathways associated with differential severity of lyme arthritis**. *J Immunol* 2006, **177**:7930-7942.
46. Hodzic E, Feng S, Barthold SW: **Assessment of transcriptional activity of Borrelia burgdorferi and host cytokine genes during early and late infection in a mouse model**. *Vector Borne Zoonotic Dis* 2013, **13**:694-711.
47. Kanno Y, Vahedi G, Hirahara K, Singleton K, O'Shea JJ: **Transcriptional and Epigenetic Control of T Helper Cell Specification: Molecular Mechanisms Underlying Commitment and Plasticity**. *Annual Review of Immunology* 2012, **30**:707-731.
48. Kuo J, Warner TF, Munson EL, Nardelli DT, Schell RF: **Arthritis is developed in Borrelia-primed and -infected mice deficient of interleukin-17**. *Pathog Dis* 2016, **74**.
49. Mandraju R, Jain A, Gao Y, Ouyang Z, Norgard MV, Pasare C: **MyD88 Signaling in T Cells Is Critical for Effector CD4 T Cell Differentiation following a Transitional T Follicular Helper Cell Stage**. *Infection and Immunity* 2018, **86**.
50. Thompson D, Watt JA, Brissette CA: **Host transcriptome response to Borrelia burgdorferi sensu lato**. *Ticks and Tick-borne Diseases* 2021, **12**:101638.
51. Whiteside SK, Snook JP, Ma Y, Sonderegger FL, Fisher C, Petersen C, Zachary JF, Round JL, Williams MA, Weis JJ: **IL-10 Deficiency Reveals a Role for TLR2-Dependent Bystander Activation of T Cells in Lyme Arthritis**. *The Journal of Immunology* 2018, **200**:1457-1470.
52. Gómez D, Diehl MC, Crosby EJ, Weinkopff T, Debes GF: **Effector T Cell Egress via Afferent Lymph Modulates Local Tissue Inflammation**. *The Journal of Immunology* 2015, **195**:3531-3536.

2.7 Figures

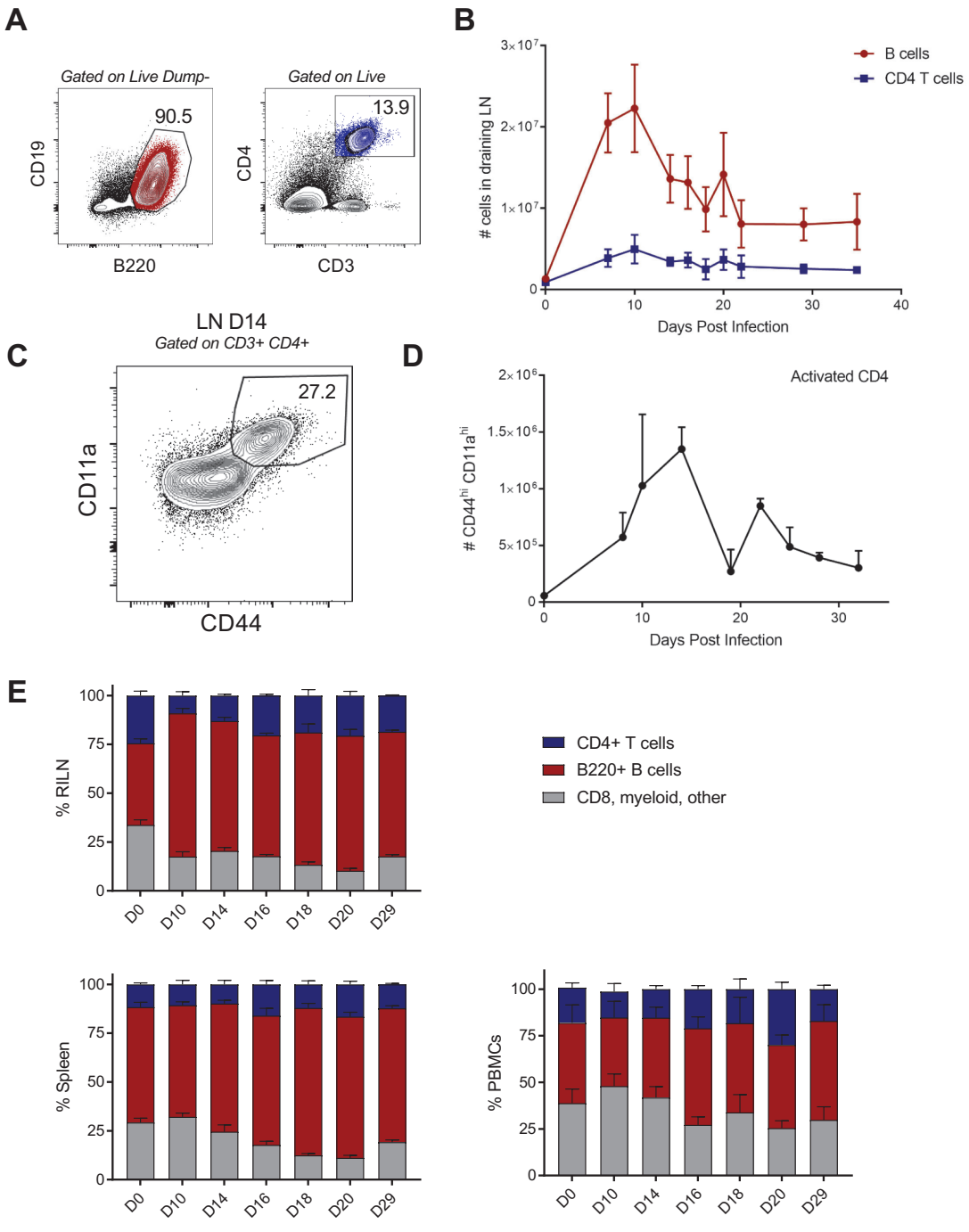
A
Gated on Live Dump-
90.5
CD19
B220
Gated on Live
13.9
CD4
CD3
B
B cells
CD4 T cells
cells in draining LN
Days Post Infection
C
LN D14
Gated on CD3+ CD4+
27.2
CD11a
CD44
D
Activated CD4
CD44hi CD11ahi
Days Post Infection
E
CD4+ T cells
B220+ B cells
CD8, myeloid, other
% RILN
% Spleen
% PBMCs
D0
D10
D14
D16
D18
D20
D29

Figure 2.1: *CD4 T cell activation and expansion during the course of Bb infection.* A) Representative FACS plots of inguinal lymph node cells of *Bb*-infected mice at 14 dpi. Shown are LN cells gated for lymphocytes, singlets, and live. B cells are also gated on dump negative (dump includes CD90+, CD4+, CD8+, NK1.1+, F4/80+). B) Total cell count of CD19+ B220+ B cells and CD3+ CD4+ T cells in the draining LN of *Bb* infected mice. C) Representative FACS plot shows gating for activated CD4 T cells ($CD44^{hi}$ $CD11a^{hi}$). D) Mean activated CD4 T cell count ± SD in draining LN of *Bb* infected mice. E) Mean frequency + SD of CD4 T cells, B cells, and other cells in draining LN, spleen, and peripheral blood of *Bb* infected mice. Data from 0, 10, 14, 22, and 29 dpi are representative of two independent experiments. Other timepoints were analyzed once. N = 4 mice at each timepoint.

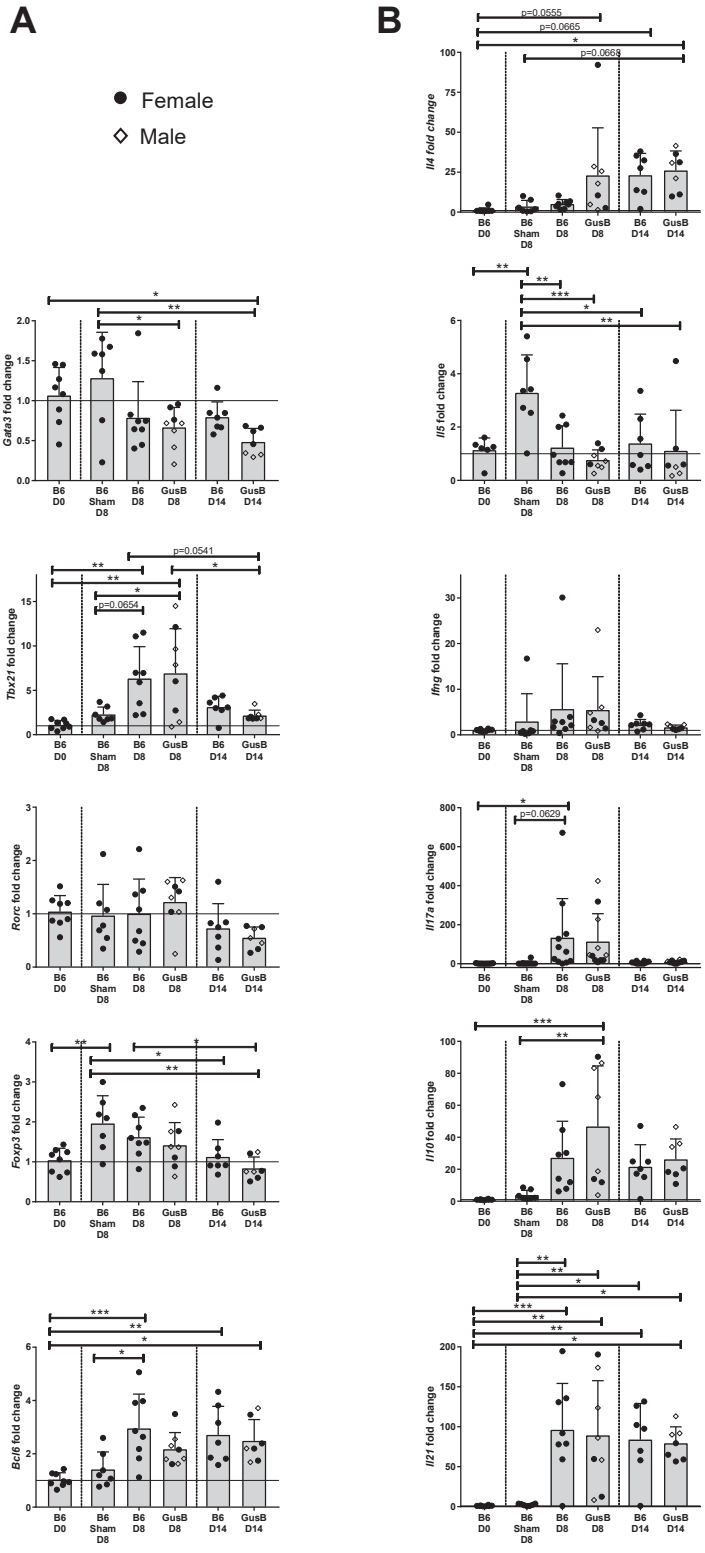
A
Female
Male
B
Gata3 fold change
Tbx21 fold change
Rorc fold change
Foxp3 fold change
Bcl6 fold change
Il4 fold change
Il5 fold change
Ifng fold change
Il17a fold change
Il10 fold change
Il21 fold change
B6 D0
B6 Sham D8
B6 D8
GusB D8
B6 D14
GusB D14
p=0.0555
p=0.0665
p=0.0668
p=0.0654
p=0.0541
p=0.0629

Figure 2.2: *CD4 T cell differentiation is dominated by Tfh rather than effector subtypes*. Bar charts show mean ± SD expression fold-changes of **A**) indicated transcription factors and **B**) cytokines among total CD4 T cells isolated from B6 and $GusB^h$ mice infected with *Bb* for 8 or 14 days, or sham-infected for 8 days, compared to non-infected B6 mice. Statistical analysis was done using one-way ANOVA with Tukey's post-hoc correction. Only significant comparisons are indicated (* $p<0.05$, ** $p<0.01$, *** $p<0.001$).

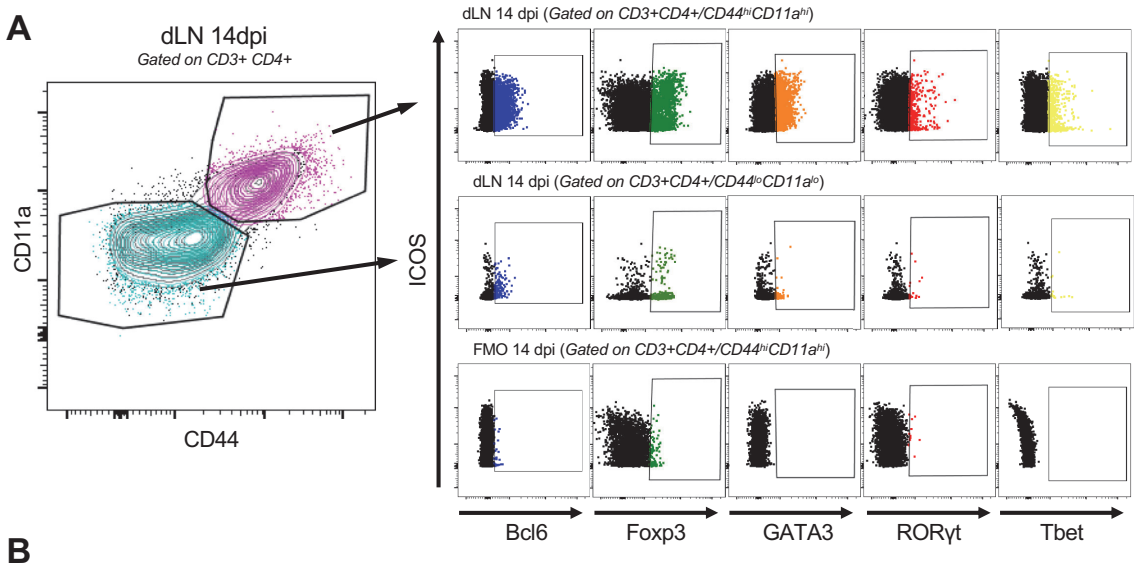
A
dLN 14dpi
Gated on CD3+ CD4+
CD11a
CD44
ICOS
dLN 14 dpi (Gated on CD3+CD4+/CD44hiCD11ahi)
dLN 14 dpi (Gated on CD3+CD4+/CD44loCD11alo)
FMO 14 dpi (Gated on CD3+CD4+/CD44hiCD11ahi)
Bcl6
Foxp3
GATA3
RORγt
Tbet

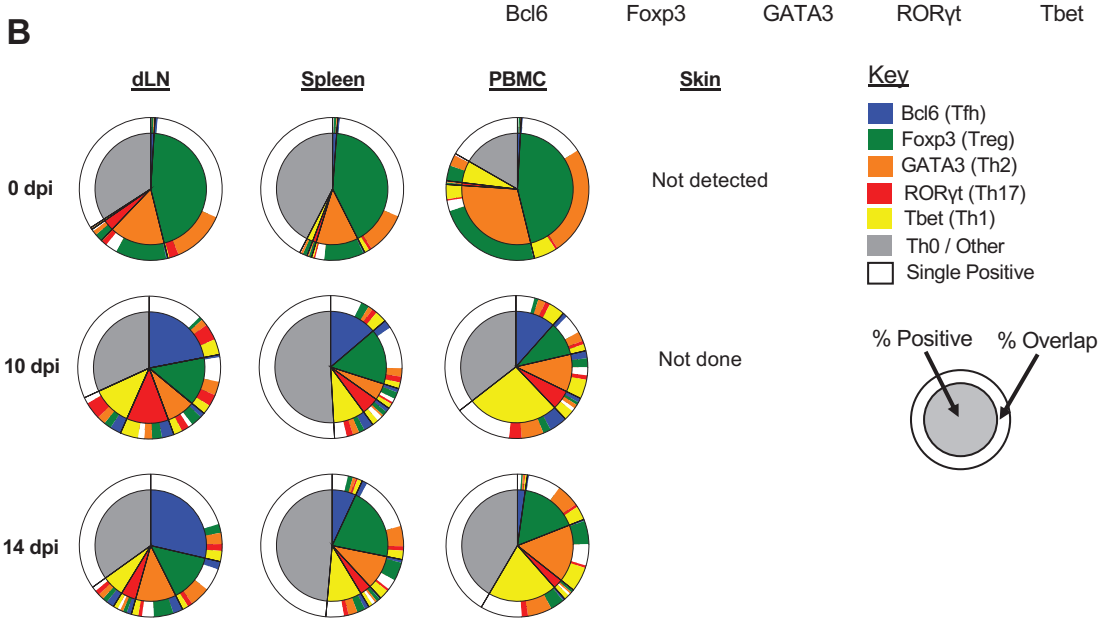
B
dLN
Spleen
PBMC
Skin
0 dpi
10 dpi
14 dpi
Not detected
Not done
Key
Bcl6 (Tfh)
Foxp3 (Treg)
GATA3 (Th2)
RORγt (Th17)
Tbet (Th1)
Th0 / Other
Single Positive
% Positive
% Overlap

Figure 2.3: *Bb-infection induces Tfh but weak CD4 effector T cell polarization.* A) Shown are representative FACS plots of inguinal lymph node cells from B6 mice 14 dpi after gating on live, single B220- CD3+ CD4+ cells (left panel). Cells were gated as activated ($CD44^{hi}$ $CD11a^{hi}$, top panels) and naïve ($CD44^{lo}$ $CD11a^{int}$, middle panels) and then analyzed for indicated transcription factor expression. Right panels indicate gating strategy for transcription factors Bcl6, Foxp3, GATA3, Rorγt, and Tbet, based on fluorescence minus one (FMO) control stains (right bottom panels) and staining of cells from gene-targeted mice (**Fig 4**). B) Pie charts indicate mean percent transcription factor positive cells among activated CD4 T cells in draining LN (dLN), spleen, PBMC and skin (interior of pie charts) at indicated times before and after *Bb* infection. Mean percent transcription factor double positive cells shown in outside ring of pie charts. Data from 14 dpi are representative of 2 independent experiments. Tissues from n=4 mice at each timepoint.

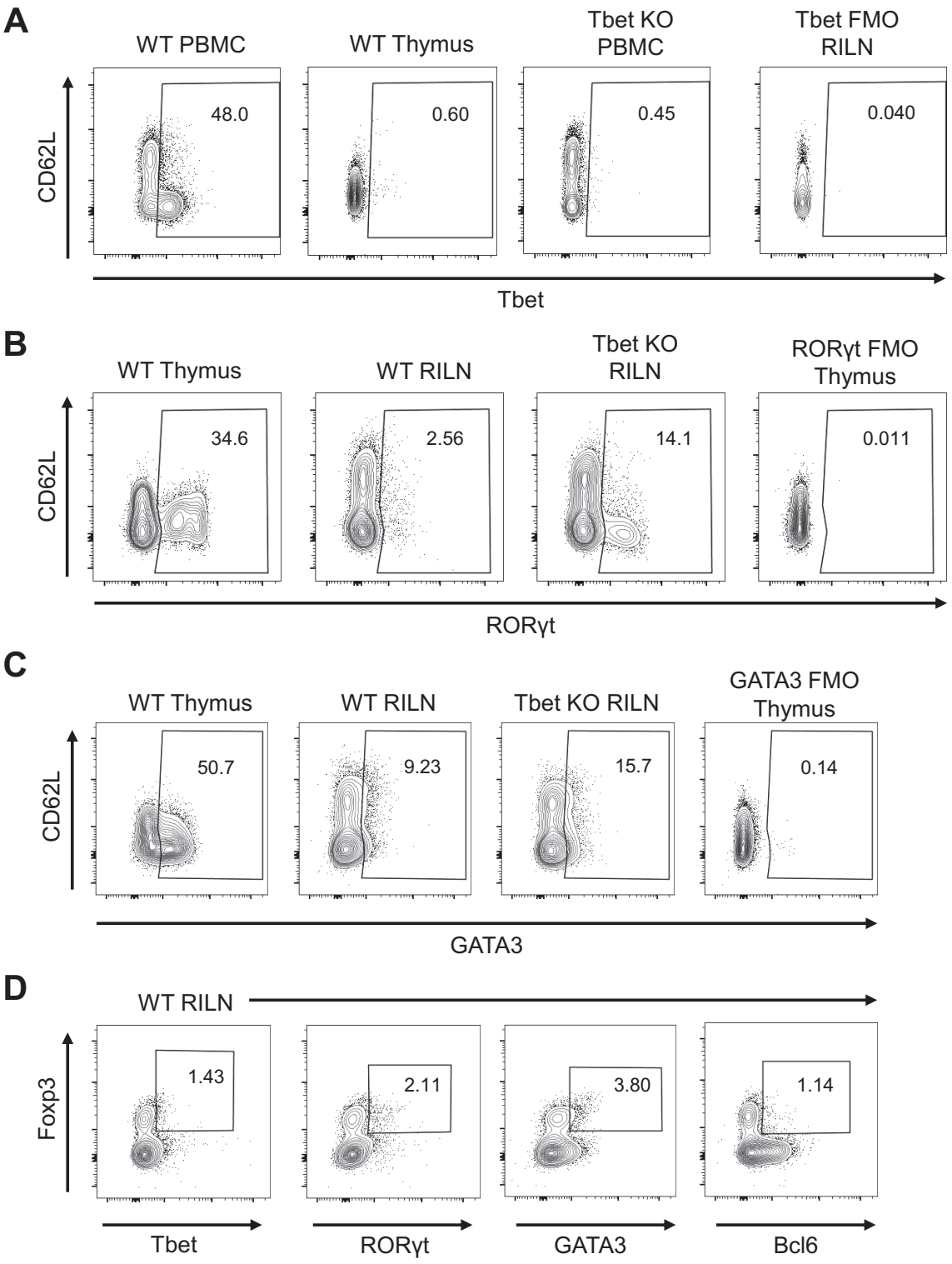
A
WT PBMC
WT Thymus
Tbet KO PBMC
Tbet FMO RILN
CD62L
48.0
0.60
0.45
0.040
Tbet
B
WT Thymus
WT RILN
Tbet KO RILN
RORγt FMO Thymus
CD62L
34.6
2.56
14.1
0.011
RORγt
C
WT Thymus
WT RILN
Tbet KO RILN
GATA3 FMO Thymus
CD62L
50.7
9.23
15.7
0.14
GATA3
D
WT RILN
Foxp3
1.43
2.11
3.80
1.14
Tbet
RORγt
GATA3
Bcl6

Figure 2.4: *Positive and negative staining controls for TFs.* A-D) Representative FACS plots of TF staining in Bb infected mice 14 dpi. All plots are gated on lymphocytes, singlets, live, CD45+ CD3+ CD4+. Draining LN (RILN) and PBMC are additionally gated on CD44hi CD11ahi. A) PBMCs are a positive control for Tbet staining. Tbet KO PBMC and Tbet FMO are negative controls. B) WT thymus and Tbet KO RILN are positive controls for RORγt staining. FMO is a negative control. C) WT thymus is a positive control for GATA3 staining. FMO is a negative control. D) Plots represent the proportion of TF+ cells that co-express Foxp3 in RILN of Bb 14 dpi mice.

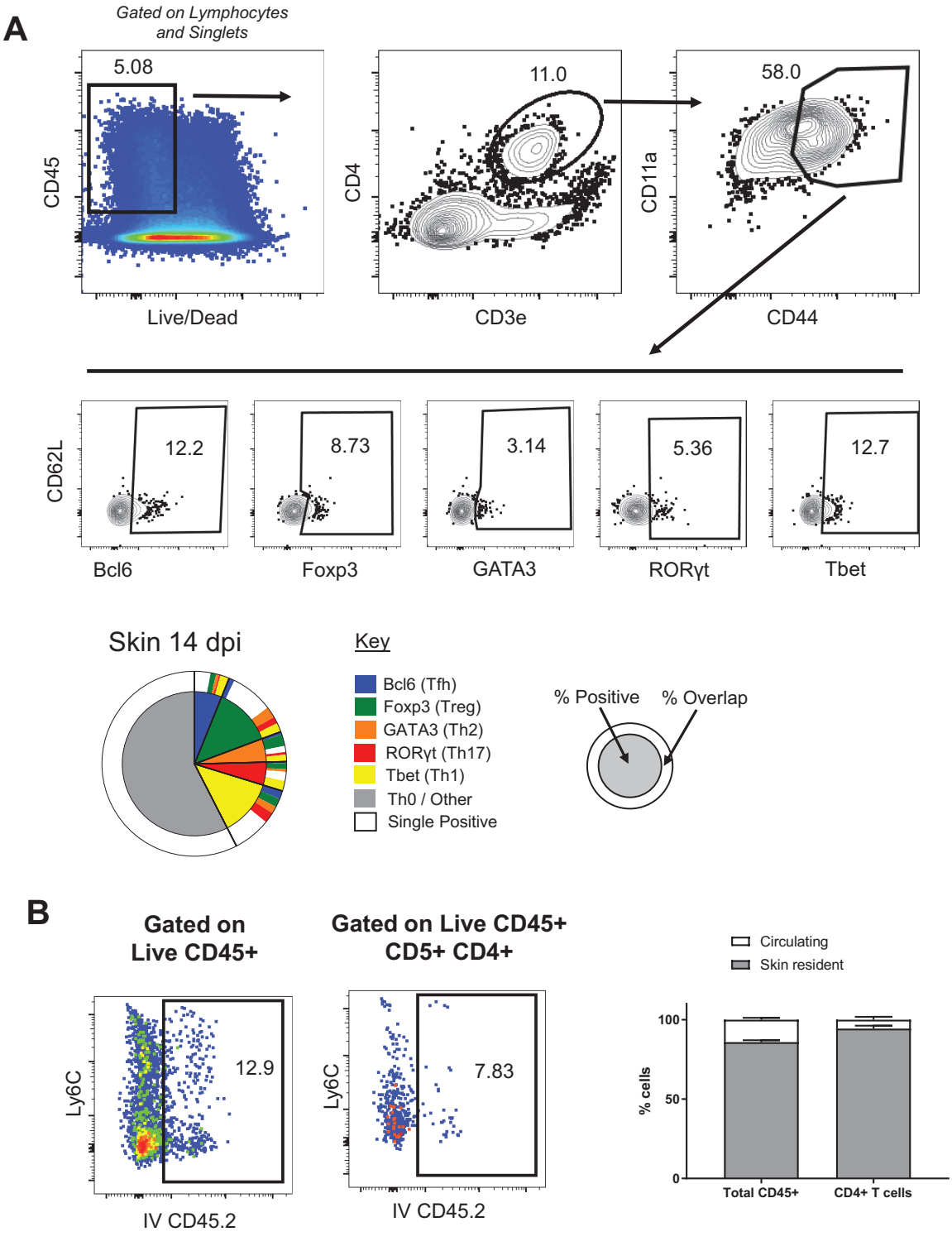
A
Gated on Lymphocytes and Singlets
5.08
CD45
Live/Dead
11.0
CD4
CD3e
58.0
CD11a
CD44
CD62L
12.2
Bcl6
8.73
Foxp3
3.14
GATA3
5.36
RORγt
12.7
Tbet
Skin 14 dpi
Key
Bcl6 (Tfh)
Foxp3 (Treg)
GATA3 (Th2)
RORγt (Th17)
Tbet (Th1)
Th0 / Other
Single Positive
% Positive
% Overlap
B
Gated on Live CD45+
Gated on Live CD45+ CD5+ CD4+
Ly6C
12.9
IV CD45.2
Ly6C
7.83
IV CD45.2
Circulating
Skin resident
% cells
100
50
0
Total CD45+
CD4+ T cells

Figure 2.5: *TF expression in skin.* A) Representative FACS plots show gating strategy for TF+ CD4 T cells in skin at 14 dpi. Pie chart shows percent TF+ activated CD4 T cells. B) Representative flow plots of skin leukocytes following intravascular labeling. Right: summary data of mean number circulating and skin resident cells ±SD. A, B) N=4 mice for each experiment, 14 dpi.

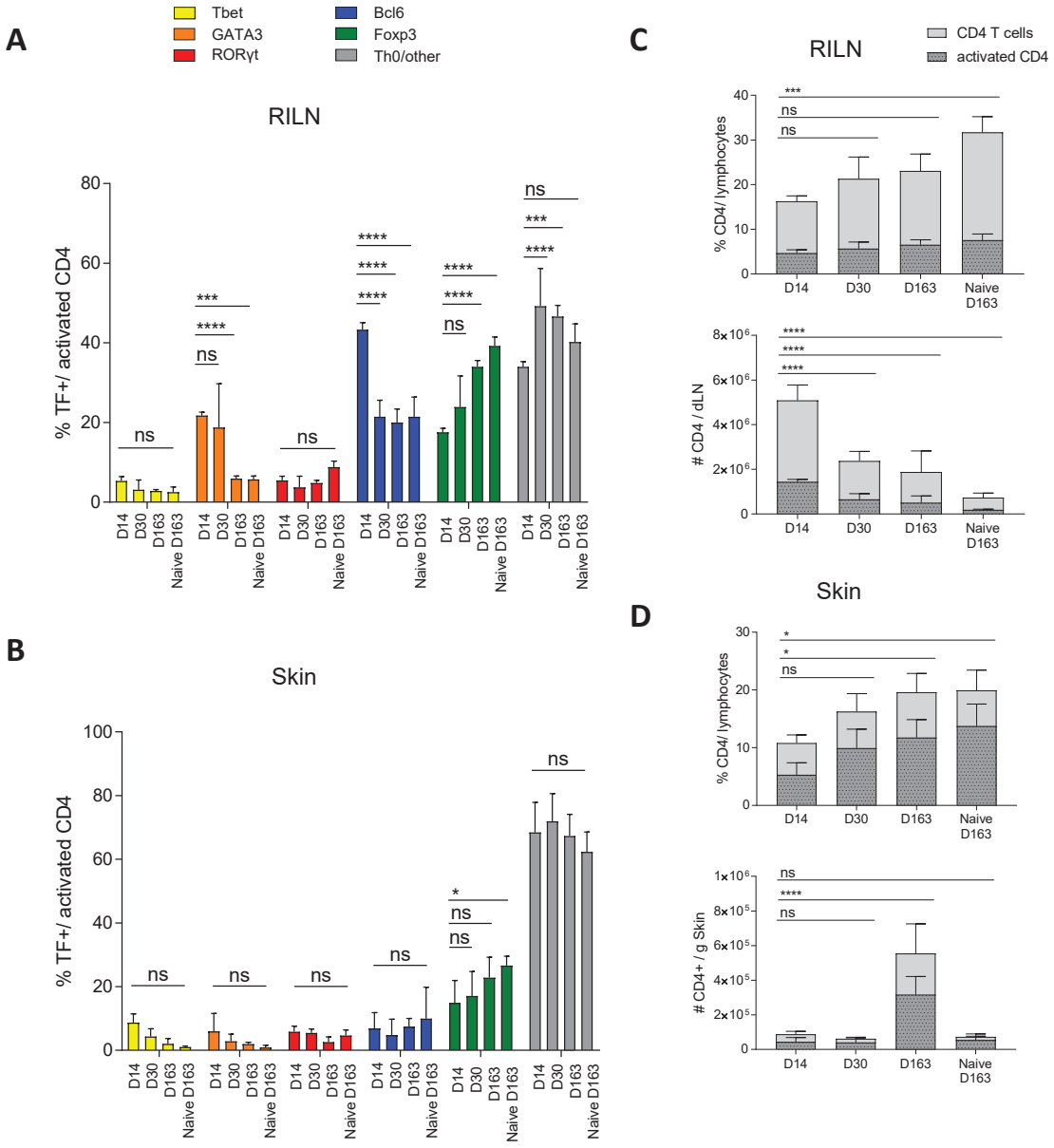
A
Tbet
GATA3
RORγt
Bcl6
Foxp3
Th0/other
RILN
% TF+/ activated CD4
B
Skin
C
RILN
CD4 T cells
activated CD4
% CD4/ lymphocytes
# CD4 / dLN
D
Skin
% CD4/ lymphocytes
# CD4+ / g Skin
D14
D30
D163
Naive D163
ns

Figure 2.6: *CD4 effector polarization does not increase with time.* A-B) Mean percent ±SD TF+ activated CD4 T cells in draining LN and skin, as well as naïve age-matched control mice (Naïve D163). C-D) Mean percent and count ± SD of total and activated CD4 T cells in dLN and skin of *Bb* infected mice. All timepoints are compared to 14 dpi using a two-way ANOVA with Tukey's post-hoc comparison (* $p<0.05$, ** $p<0.01$, *** $p<0.001$, ****$p<0.0001$). Data pooled from 4 independent experiments; n = 3-7 mice for each group.

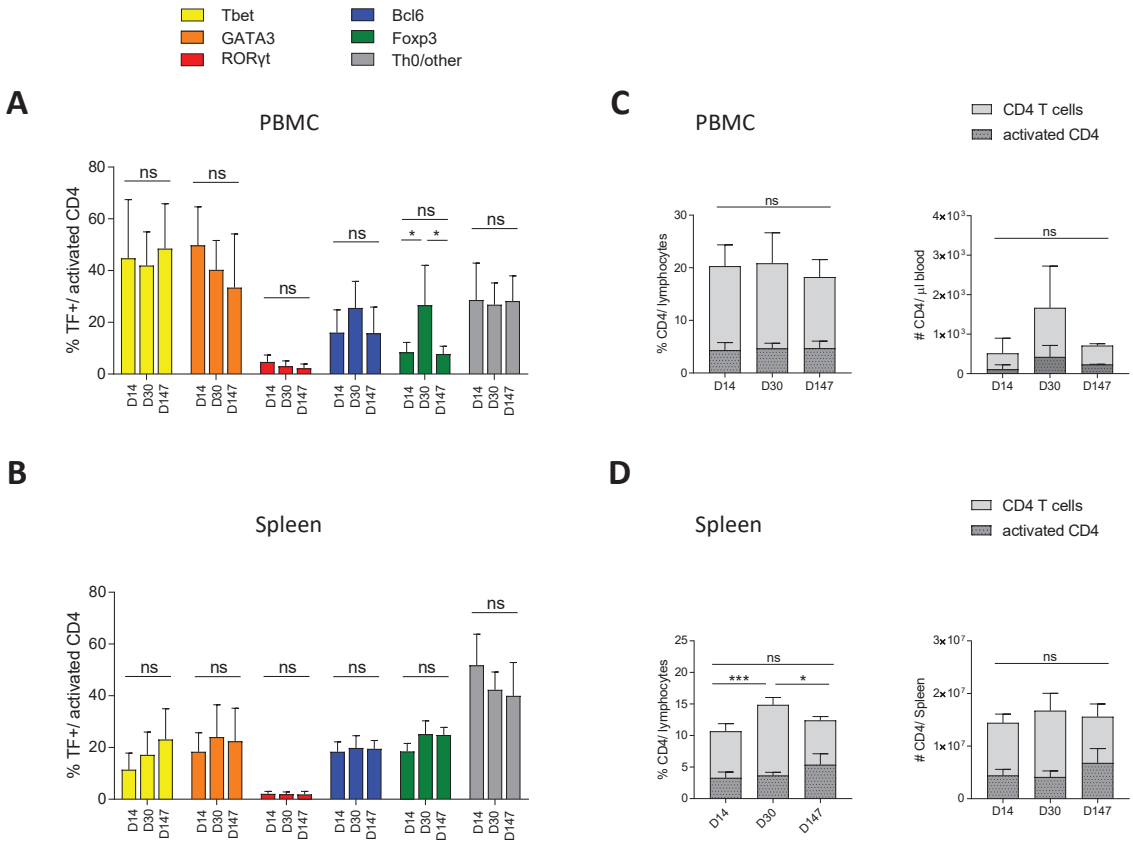

Figure 2.7: *Lack of effector CD4 polarization in PBMC and spleen.* A-D) Mean ± SD CD4 T cells in PBMC and spleen in acute and chronic Bb infection. Two-way ANOVA with Tukey's post-hoc comparison (* $p<0.05$, ** $p<0.01$, *** $p<0.001$).

Chapter 3

Generation of a pMHCII tetramer for the identification of *Borrelia burgdorferi* specific CD4 T cells in C57BL/6 mice

3.1 Abstract

CD4 T cells are central regulators of both cellular and humoral immune responses to infections. Yet, understanding of the induction kinetics, quality, and effectiveness of CD4 T cell responses to Borrelia burgdorferi (Bb), the causative agent of Lyme disease, are limited. Generation and use of MHC class II "tetramers", peptide-loaded MHCII multimers that can bind to peptide-specific CD4 T cells, has significantly enhanced our ability to interrogate CD4 T cell responses by flow cytometry, but no such reagents are available to study CD4 T cell responses to Bb in C57BL/6 mice. Here I describe the identification of an immunogenic, I-A^b restricted CD4 T cell epitope ($Arp_{152-166}$) on Arthritis related protein (Arp), a constitutively expressed Bb surface antigen that we had shown previously to induce strong T-dependent IgG responses to infection in mice. I then validated that an I-A^b tetramer generated with this peptide identified Arp-specific CD4 T cells *ex vivo*, in lymph nodes of *B. burgdorferi*- but not *B. afzelii*-infected, or non-infected C57BL/6 mice. Furthermore, I demonstrate that *in vitro* cultures of lymph node cells stimulated with recombinant Arp led to strong proliferation among tetramer stained CD4 T cells. In a proof-of-concept study assessing the usefulness of this reagent for the analysis of Bb-specific CD4 T cell function, I demonstrate that Arp-specific CD4 T cells are preferentially differentiating into T follicular helper (Tfh) and T follicular regulatory (Tfr) cells on day 14 after infection, consistent with the previously observed induction of strong serum Arp-specific IgG responses. Together, this study provides a new tool for the interrogation of CD4 T cell responses to Bb.

3.2 Introduction

Borrelia burgdorferi (Bb), a spirochetal bacterium, causes Lyme disease in a variety of species, including humans [1], but causes persistent non-resolving infection with few if any disease manifestations in small birds and rodents, considered "reservoir species" [2,3]. Bb is transmitted to humans by the bite of adult blacklegged ticks of the order Ixodes. Infection of ticks with Bb requires the presence of chronically infected reservoir hosts, as there is no vertical transmission of Bb from adult ticks to eggs [4]. A number Bb immune evasion mechanisms have been identified that support the establishment of chronic infection in these species. Among them is the differential expression of immunogenic Bb surface antigens. Differential expression of Bb antigens plays an important role in the complex life cycle of Bb, allowing the spirochete to evade antibody-mediated immunity in order to establish persistent infection [5]. One apparent example is the expression of the outer surface protein (Osp) C by tick-dwelling Bb. While expression of OspC is required for infection of a mammalian host, once infection occurs, OspC is rapidly downregulated, explaining the rather modest IgG titers observed to OspC in C57BL/6 mice following experimental infection [6]. Bb engineered to constitutively express OspC were rapidly eliminated from infected mice [7], further demonstrating the importance of dynamically regulating OspC expression for Bb persistence.

Bb also expresses the variable lipoprotein E (vlsE), which through the use of various gene expression cassettes alters its antigenic surface profile following infection, allowing Bb to evade antibody-mediated immunity [8]. It has been proposed that expression of vlsE on the surface of Bb acts also as a "shield" that prevents recognition of other immunogenic surface antigens by the B cell response [9]. Specifically, it was shown that the absence of vlsE expression could cause clearance of Bb infection in mice that were given antibodies to the surface antigen "arthritis related protein" (Arp) [9].

Arp is a surface lipoprotein that is constitutively expressed throughout infection of mice [10,11]. Although its function is unknown, its absence diminishes the infectivity of Bb spirochetes [12]. Anti-Arp immune serum was shown to induce arthritis resolution in arthritis-susceptible strains of mice, but it did not induce bacterial clearance [13,14]. Furthermore, we previously showed that anti-Arp IgG responses are highly prevalent in C57BL/6 mice infected with Bb N40, and that the induction of anti-Arp IgG required the presence of CD40L and CD4 T cells [15,16], thus cognate T dependent B cell activation. Despite the T-dependence of the anti-Arp response, antibiotic treatment rapidly reduced anti-Arp IgG serum titers to background levels, strongly suggesting a failure of the anti-Arp response to induce long-lived plasma cells (LLPC). In support of this, we were unable to detect Arp-specific LLPC in the bone marrow of Bb-infected mice for over 3 months [17]. Furthermore, we demonstrated a rapid collapse of germinal centers [17], the structures responsible for the induction of LLPC, suggesting that the anti-Arp response is functionally defunct, but the reason for this defective immune response remains to be established.

Because there are currently no tools available with which to assess Bb-specific CD4 T cell responses and only one human CD4 epitope has been characterized previously [18], we conducted the following study to identify MHCII I-A^d-restricted CD4 T cell epitopes and to test their utility for inclusion in a MHCII I-A^b "tetramer" for Bb infection studies with C57BL/6 mice.

3.3 Results and Discussion

High degree of sequence conservation of arthritis-related protein (Arp) among *B. burgdorferi sensu stricto* strains

Studies on antigen-specific CD4 T cell responses in the context of a polyclonal T cell response have been made possible through the generation of MHCII-peptide complexes that when multimerized can be used

to label CD4 T cells for analysis by flow cytometry. We aimed here to develop an MHCII-restricted tetramer as a tool to study Bb-specific CD4 T cell responses in C57BL/6 mice, the most common laboratory strain of mice used today. We evaluated the Arp protein of Bb N40 as a candidate target, because we had shown previously that Arp is highly immunogenic and induces a strong, T-dependent IgG response in Bb N40-infected C57BL/6 mice [19]. Thus, suggesting the presence of MHCII-restricted epitope(s) on the Arp protein. To determine whether the use of Arp may also allow studies of T cell responses to other Bb strains we performed a basic local alignment search tool (BLAST) search for the *arp* gene from Bb strain N40 (accession NC_017415.1, locus tag BBUN40_RS05425). We identified at least eight strains of *B. burgdorferi sensu stricto*, including two commonly used laboratory strains, B31 and N40, that contained the *arp* gene (**Table 3.1**). Comparison of the Bb Arp protein sequences revealed a high degree of homology across all Arp sequences (>90%). Notably, strain B31 was among the five Bb strains that shared an identical Arp sequence with N40. In contrast, the closely related *Bb sensu lato* strains, *B. afzelii* and *B. garinii* (Refseq accession GCF_000222835.1 and GCF_003814405.1, respectively) lacked Arp (**Table 3.1**). Due to the high immunogenicity and sequence conservation of *arp*, we proceeded to identify Arp-specific I-A^b-restricted epitopes on Bb N40.

Arp contains a strong I-A^b-restricted epitope that induces CD4 T cell responses in C57BL/6 mice after infection with Bb N40.

To identify I-A^b-restricted epitopes on the Arp protein, we used total CD4 T cells enriched from the peripheral lymph nodes (LN) of day 12 Bb-infected C57BL/6 mice as a source of Arp-specific T cells, as this resulted in optimal detection of cytokine secretion via ELISPOT. We generated 20-mer peptides that spanned residues 8 through 332 of Arp (NCBI accession WP_010890266.1[*]). To assess the presence of these cells we co-cultured enriched CD4 T cells with irradiated, total spleen cells from non-infected

[*] The Arp protein was originally annotated as "ErpD."

C57BL/6 mice in the presence of individual 20-mer peptides from a library of Arp peptides (20-mer peptides offset by 5 amino acids). Since the CD4 T cell response to Bb is considered Th1 dominant [20-22], we first used IFNγ ELISPOT as a read-out of CD4 T cell activation following restimulation with either whole recombinant (r)Arp or individual Arp peptides. Controls were mediastinal lymph node CD4 T cells from day 7 influenza A/Puerto Rico/8/34 (A/PR8)-infected mice stimulated with heat-inactivated A/PR8. While these controls gave robust increases in IFNγ ELISPOTs when compared to the negative control wells that lacked peptide additions (**Fig. 3.1A**), stimulation of CD4 T cells enriched from Bb-infected mice with rArp or peptides resulted in an at best very modest induction of IFNγ ELISPOTS (**Fig. 3.1A**). Similar results were obtained also when we isolated CD4 T cells from mice infected with Bb via syringe inoculation, as well as mice infected with tissue adapted spirochetes for one year (data not shown). Thus, the failure to measure IFNγ ELISPOTs after Arp stimulation was unlikely due to technical difficulties with the IFNγ ELISPOT or the route of infection, and was unlikely due to the time point at which we harvested the T cells. Furthermore, given that we previously showed the presence of activated CD4 T cells in the lymph nodes of Bb infected mice on day 12 after infection [16,17], our data suggested that Bb infection did not induce IFNγ-producing CD4 T cells in the lymph nodes, although it is possible IFNγ producing cells may exist in other tissues. Since IL-2 is secreted by CD4 T cells following TCR engagement [23], we proceeded to assess IL-2 ELISPOT generation in these cultures instead. The drawback in using IL-2 as a readout for TCR engagement is the potential for higher background in ELISPOT assays due to naïve T cell's ability to secrete IL-2 [24]. To overcome this limitation, we calculated the fold-change of spots obtained from peptide stimulated wells compared to the mean number of spots seen in the PBS control wells. Using this approach, we found that stimulation of lymph node cells with rArp consistently resulted in robust IL-2 ELISPOT-induction compared to the control wells (**Fig. 3.1B**). Screening the Arp peptide library at least 3 times resulted consistently in strong increases in IL-2 ELISPOTS above background in cultures containing peptide fragments F22 and F23, and less strong induction in ELISPOTs from additional Arp regions (**Fig. 3.1B**).

In order to more precisely identify the specific Arp epitope, we next generated shorter 15-mer peptides offset by 5 amino acids, representing regions of interest from our initial screen. In this analysis we focused on Arp regions F22-23 and others that had resulted in more variable increased IL-2 ELISPOTs. The highest number of IL-2 ELISPOTS were induced by a 15-mer peptide "B11", which shared overlapping amino acid sequences with peptides F22 and F23 (**Fig. 3.1C**). No other peptide induced significant and reproducible IL-2 ELISPOTs (**Fig. 3.1C**). This suggested the presence of at least one T cell epitope in this region of Arp.

To more precisely determine the epitope sequence included in peptide B11, we next screened the original B11 15-mer peptide as well as additional peptides generated by including 1, 2 or 3 amino acid residues upstream (-1, -2 and -3), or downstream (+1, +2 and +3) of the B11 sequence. T cell stimulation via B11 (+3), spanning Arp residues 152 to 166, resulted in the largest number of IL-2 ELISPOTs. The spot counts were comparable to those observed with the full length rArp, suggesting that we identified a major, if not the only I-A^b-restricted epitope on Arp (**Fig. 3.1D, E**). As little as 5ng of $Arp_{152\text{-}166}$ induced significant increases in IL-2 ELISPOTs compared to PBS (**Fig. 3.1F**), indicating the high immunogenicity of this peptide. Consistent with induction of ELISPOTs by peptides F22 and F23, the $Arp_{152\text{-}166}$ sequence spanned these originally identified immunogenic regions (**Fig. 3.1G**).

Generation and validation of an I-A^b restricted Arp Tetramer

Due to the low affinity nature of TCR interactions with soluble peptide-MHC class II (pMHCII) molecules, tetrameric pMHCII molecules have been developed in order to identify CD4 T cells expressing antigen-specific TCRs [25]. MHC class II tetramers have proved invaluable in following CD4 T cell responses in non-TCR transgenic models of infection and immunization [26]. Using the above

$Arp_{152-166}$ (TIDFYIEPRPISSFL) peptide, the NIH Tetramer Core Facility generated two MHCII ($I\text{-}A^b$) peptide "tetramer" complexes, one labeled with PE the other with BV421. Using dual staining with these tetramers, approximately 0.05 – 0.2% of CD4 T cells in the draining inguinal LN of Bb infected mice at the height of their response, 14 days post infection, stained with both tetramers (**Fig. 3.2A**). Single stained cell population likely constitute non-specific binding to non-peptide components of the tetramer. To determine whether we could further optimize the identification of Arp-specific CD4 T cells with these tetramers, we treated cells with Dasatinib, a protein kinase inhibitor (PKI). PKI treatment is thought to increase the number of TCR molecules retained on the cell surface, increasing tetramer binding and staining intensity [27], i.e. enhancing the mean fluorescence intensity (MFI) of the tetramer-bound cells [27,28]. As expected, PKI treatment did not affect the number of cells that bound the Arp tetramer (**Fig. 3.2B**). It did, however, result in modest increases in the MFI of the PE-but not BV421-labeled tetramer (**Fig. 3.2C**). We therefore treated all subsequent samples with PKI prior to tetramer labeling.

We then conducted several studies to confirm that the Arp tetramer identified Bb-induced antigen-specific CD4 T cells. First, we tested further whether the Arp-tetramer identifies Bb infection induced CD4 T cells. After staining lymph node cells from Day 14 Bb-infected mice as well as controls with PE-labeling Arp-tetramers and anti-PE antibodies conjugated to magnetic beads, we performed a magnetic pull-down assay using a magnetic column (**Fig. 3.3A**). The pull down resulted in an at least 50-fold increase in the frequency of Arp-specific CD4 T cells among total lymph node lymphocytes from day 14 Bb infected mice, compared to frequencies measured prior to enrichment (2.55% ± 0.41% vs. 0.0492% ± 0.0066%, respectively; **Fig. 3.3B**). In contrast, use of lymph node cells from naïve mice, resulted in only a modest enrichment in the number of Arp-specific CD4 T cells (**Fig. 3.3B**). Presumably these cells constituted the Arp-specific CD4 T cells of the naïve repertoire. Their frequencies (0.0129% ± 0.0113% of total tetramer-enriched lymphocytes, **Fig. 3.3B**), is similar to precursor frequencies reported with other systems by others [29-31].

To ensure that infection did not lead to an increased in "stickiness" or non-specific expansion of tetramer-binding cells, we quantified Arp tetramer stained CD4 T cells also in mice infected with the *B. afzelii* strain pKo, a spirochete which is closely related to *B. burgdorferi*, but lacks *arp* (**Table 3.1**). *B. afzelii* infection induced a CD4 response of similar magnitude to that induced by Bb 14 dpi in the draining LN (3.3-fold increase in total number of CD4 vs. 3.8-fold increase, respectively, compared to naïve LN—data not shown). Yet, the total number of Arp tetramer binding CD4 T cells detectable in these mice was not significantly different in non-infected controls, nor did they differ from the number of CD4 T cells that bound to two control tetramers of irrelevant specificity in Bb infected LN (**Fig. 3.3C**). These data strongly suggested that $Arp_{152-166}$ tetramer-bound CD4 T cells recognize a Bb-specific antigen and expand in response to infection with Arp-expressing but not Arp non-expressing spirochetes. A Bb-specific expansion of $Arp_{152-166}$ -specific CD4 T cells was further supported by data showing that >80% of Arp-tetramer positive CD4 T cells were enriched for T cells expressing an activated ($CD44^{hi}$ $CD11a^{hi}$) phenotype (**Fig. 3.3D**).

Together, these data demonstrate that the I-A^b tetramer displaying Bb $Arp_{152-166}$ reliably identifies Bb-specific CD4 T cells generated during infection with Arp-expressing but not Arp non-expressing *Borrelia* spirochetes. The increased number of Arp-specific CD4 T cells detectable 14 dpi compared to either uninfected mice, or mice infected with a Borrelia strain lacking Arp, demonstrates furthermore that the tetramer-binding sCD4 T cells undergo clonal expansion *in vivo* in a Bb-specific manner.

In vitro rArp stimulation leads to enrichment of $Arp_{152-166}$ specific T cells

Final validation of the specificity of the $Arp_{152-166}$ tetramer was done by stimulating total lymph node cells harvested from Bb infected and non-infected mice with recombinant (r)Arp for 6 days after first labeling

these cells with a proliferation dye. As expected, stimulation with rArp resulted in robust proliferation of CD4 T cells from Bb infected mice, with higher frequencies of divided CD4 T cells and a larger total number of CD4 T cells compared to cultures from uninfected mice, as well as control wells without rArp (**Fig. 3.4A**). Moreover, comparison of rArp-stimulated versus non-stimulated lymph node cultures showed a strong expansion of Arp tetramer-binding CD4 T cells over a 7-day culture period (**Fig. 3.4B**). All tetramer-binding CD4 T cells from rArp stimulated cultures had lost their proliferation dye signal, indicating extensive cell divisions. Thus, we conclude that the $Arp_{152-166}$ tetramer identifies Arp-specific CD4 T cells induced as part of a polyclonal CD4 T cell response to Bb N40 infection of C57BL/6 mice.

Polarization and function of Arp-specific CD4 T cells

Given the somewhat surprising lack of IFNγ producing CD4 T cells observed in our initial ELISPOT assays, we aimed to characterize CD4 T cell polarization during Bb infection and to compare Arp-specific CD4 T cells to the total pool of activated ($CD11a^{hi}$ $CD44^{hi}$) CD4 T cells. To this end, we developed multicolor flow cytometric intracellular staining panels with which to study simultaneously the expression of five lineage-defining transcription factors (Bcl6, FoxP3, Tbet, GATA-3 and RORγt) in conjunction with cell surface markers as well as dual tetramer staining **Fig. 3.5A**). Staining of thymocytes confirmed our ability to stain for each of these transcription factors (data not shown). The results of this analysis demonstrated that the overall expression pattern of transcription factors responsible for effector T cell polarization (Tbet, GATA3, RORγt, supporting polarization towards a Th1, Th2 and Th17 state, respectively) was overall similar between Arp-specific and Arp non-specific CD4 T cells (**Fig. 3.5B**). Consistent with our functional analysis measuring IFNγ secretion by ELISPOT, Tbet-expressing and thus Th1 polarized CD4 T cells were rare in lymph nodes of Bb-infected mice. There was, however, a small increase in the frequency of Tbet-expressing CD4 T cells among the Arp+ cells, although this difference did not reach statistical significance. We further noted that of the Tbet-expressing CD4 T cells fewer than 25% expressed solely Tbet. Rather, most co-expressed additional transcription factors, notably Bcl6 and

FoxP3, among both the Arp-specific and the Arp non-specific cells (**Fig. 3.5C**). Similarly, about 75% of GATA3+ and RORγt+ CD4 T cells expressed at least one additional transcription factors, and the frequencies of cells expressing these factors was overall remarkably low (**Fig. 3.5A**). No major difference in polarization signature of effector T cells was observed between Arp-specific and Arp non-specific cells (data not shown). We conclude that Arp-specific CD4 T cells lack strong effector polarization.

However, Arp-specific CD4 T cells did exhibit significant expression of Bcl6, the canonical transcription factor of Tfh cells, which are involved in T-dependent (TD) B cell responses. Moreover, the Arp+ CD4 T cells showed a significantly higher frequency of Bcl6+ cells compared to the Arp non-specific cells (**Fig. 3.5B**). This finding is consistent with previous experiments that identified Arp as inducing strong T-dependent IgG responses after Bb infection. In contrast to the findings in CD4 T cells with mixed expression of transcription factors associated with effector polarization, only a relatively small fraction of Bcl6+ cells expressed additional transcription factors (**Fig. 3.5E**). Of these, the most notable were the Tfr cells that coexpressed Bcl6 and FoxP3 (**Fig. 3.5D**). The frequency of Tfr cells was significantly higher among Arp-specific CD4 T cells, resulting in a higher ratio of Tfr:Tfh among the Arp-specific cells compared to those not binding Arp (**Fig. 3.5F**). Consistent with these results, analysis of all Bcl6+ CD4 T cells showed a significant enrichment for Arp-specific FoxP3+ Treg cells (**Fig. 3.5G**). These data are interesting, as Tfr cells have been shown previously to constrain GC responses in some contexts [32,33]. Given our previous findings of a rapid collapse of GC after Bb infection, assessing whether the increased frequencies of Tfr among Arp-specific CD4 T cells may constrain the Arp-specific GC response is a future goal of our studies. Similarly, the biological significance of the apparent lack of strong CD4 T cell effector polarization in the lymph nodes of Bb infected mice remains to be further evaluated.

In conclusion, we have identified an immunogenic MHCII I-A^b restricted epitope on a constitutively expressed and highly conserved Bb surface antigen that is recognized by about 0.05% of activated lymph node CD4 T cells at the height of the lymph node response. MHC II tetramers containing the identified Arp peptide stained Bb-specific T cells that showed a surprising lack of strong effector T cell polarization, but instead expressed Bcl6 either alone or in combination with FoxP3, thus identifying Tfh and Tfr, respectively. The lack of effector polarization that I described in Chapter 2 is unlikely to be explained by our previous inability to distinguish bystander activated from Bb-specific CD4 T cells, since the overall transcription factor expression profile was similar between the Arp-specific CD4 T cells compared to the overall CD4 T cell response.

3.4 Materials and Methods

Mice and infections

C57BL/6 (000664) and B6.Cg-*Prkdc*^{scid}/SzJ (B6-SCID, 001913) mice were purchased from The Jackson Laboratories, and housed under specific pathogen free conditions. To generate tissue-adapted spirochetes [15,17], B6-SCID mice were injected intradermally with 1 x 10^5 low passage cultured N40 Bb spirochetes in the intrascapular region of the dorsal midline. After at least 14 days of infection, ear tissue from B6-SCID mice was transplanted subcutaneously in the right rear hock of 8 – 12 weeks old recipient female C57BL/6 mice, leading to their infection. This mode of infection ensured that the right inguinal lymph node was always the infection-site draining lymph node. At various times after infection mice were euthanized by overexposure to CO_2 prior to harvesting tissues. All procedures were performed in strict accordance with protocols approved by the Animal Care and Use Committee of University of California, Davis.

Peptide libraries

Peptides representing 20 mer fragments overlapping by 5 amino acids covering residues 8 through 332 of the Arp sequence (NCBI reference WP_010890266.1) were generated by Genscript. 15 mer peptides overlapping by 5 amino acids were subsequently generated of regions of interest (approximately 40% of the Arp sequence). Individual lyophilized peptides were reconstituted according to manufacturer's instructions, using either water, or water mixed with ammonium hydroxide (NH_4OH), DMSO, or acetic acid (C_3HCOOH). PBS served as a no peptide control.

ELISPOT

96-well ELISPOT plates were coated with anti-IFNγ (clone AN-18, eBioscience) or anti-IL-2 (clone JES6-1A12, eBioscience) in PBS overnight, and blocked with 4% BSA as described previously [17]. CD4 T cells from the draining lymph nodes of 12-day Bb infected mice were enriched by magnetic separation. Single cell suspensions of spleen cells from non-infected congenic mice were irradiated (3000 rad) and served as feeder cells. 1×10^5 CD4 T cells and 4×10^5 irradiated splenocytes were plated in each well, resuspended in RPMI culture media supplemented with 10% fetal calf serum. Varying concentrations of recombinant protein, peptide, or heat inactivated influenza A/Puerto Rico 8/34 virus were added for overnight culture at 37 C in 5% CO_2. Cytokine detection antibodies were added following lysis of the cells using water. Biotinylated anti-IFNγ (clone R4-6A2, eBioscience) or anti-IL-2 (clone JES6-5HA, eBioscience) and streptavidin conjugated to alkaline phosphatase (BD Pharmingen) was used to label secreted cytokines and spots were revealed using nitro-blue tetrazolium chloride (NBT)/ 5-bromo-4-chloro-3'-indolyphosphate p-toluidine salt (BCIP) substrate (Thermo Fisher). Spots were imaged and enumerated using an iSpot Spectrum EliSpot Reader System (Advanced Imaging Devices GmbH). Results were expressed as fold-change over control wells receiving PBS instead of protein or peptide.

Flow Cytometry

As described previously [17,34], lymph nodes and other tissues were dissociated between frosted glass slides and passed through a 70 μm nylon mesh filter to create single cell suspensions. If erythrocyte contamination was visible, single cell suspensions were treated with ammonium chloride potassium (ACK) lysis buffer for 60 seconds, then washed with staining media. Cell concentration was determined by hemacytometer count. Prior to antibody labeling, cells were treated with anti-CD16/CD32 (Fc block generated in-house; clone 2.4G2) and labeled with LIVE/DEAD Fixable Aqua Dead Cell Stain Kit (Invitrogen) for discrimination of live vs. dead cells. Cells were then stained with combinations of the following antibodies (*conjugate clone manufacturer*): CD3 (Alexa700 500A2 Invitrogen, PerCP-ef710 17A2 Invitrogen, FITC 2C11 in house), CD4 (Alexa700 RM4-5 Invitrogen, BUV395 RM4.5 BD Biosciences, APC-ef780 GK1.5 Invitrogen), CD19 (BV786 ID3 BD Biosciences, PE-CF594 ID3 Invitrogen, BV650 ID3 BD Biosciences), B220 (FITC RA3-6B2 in house), CD44 (BV711 IM7 Biolegend), CD11a (PE M17/4 Invitrogen, Cy7-PE 2D7 BD Biosciences), ICOS (BUV395 C398.4A BD Biosciences, BV786 C398.4A Biolegend), PD-1 (APC-ef780 J43 Invitrogen), CD8a (BUV737 53-6.7 BD Biosciences, AF700 53-6.7 Invitrogen), NK1.1 (Alexa700 PK136 Invitrogen), Gr-1 (red fluor 710 1A8 Tonbo), F4/80 (Alexa700 BM8 Biolegend), Bcl6 (Alexa647 K112-91 BD Biosciences), Foxp3 (FITC FJK-16s Invitrogen), GATA3 (PE-Cy5 TWAJ Invitrogen), RORγt (PE-CF594 Q31-378 BD Biosciences), Tbet (Cy7-PE 4B10 Invitrogen). Extracellular labeling was performed on ice for 20 minutes. For intracellular labeling, cells were fixed and permeabilized with Foxp3 Transcription Factor Staining Buffer Set (eBioscience 00-5523-00) following manufacturer's instructions. Intracellular antibodies were incubated for 30 minutes at room temperature. Data was acquired on either a LSRFortessa or FACSymphony flow cytometer (BD), and analyzed using FlowJo software.

Protein Kinase Inhibitor (PKI) treatment

PKI treatment of single cell suspensions to enhance tetramer staining was performed as described previously [27]. Briefly, a stock solution of Dasatinib (Selleck Chemical) was diluted to 1 mM in DMSO and stored at -20 C. Lymph node single cell suspensions were incubated with a final concentration of 50 nM Dasatinib in PBS at 37 C for 30 minutes. Cells were washed twice with staining media before proceeding to tetramer incubation and additional antibody labeling as outlined for flow cytometry.

$Arp_{152-166}$ Class II tetramer labeling

I-A^b restricted $Arp_{152-166}$ MHC II tetramers conjugated to phycoerythrin and BV421 were generated by the NIH Tetramer Core. Following PKI treatment of lymph node single cell suspensions, $Arp_{152-166}$ tetramers were incubated with cells for 60 minutes at room temperature and washed with staining media before proceeding to further labeling as outlined under flow cytometry.

***In vitro* stimulation assay**

Lymphocytes were harvested from the right inguinal (draining) lymph node of Bb infected mice at 21 dpi, or mixed peripheral lymph nodes of age-matched uninfected controls. Cells were incubated with 1.25µM of CellTrace Far Red proliferation dye (Invitrogen) diluted in PBS, for 10 minutes at 37 degrees C, then washed twice with staining media. Cells were resuspended in RPMI (Gibco) culture media containing 10% FBS (Gibco), 100 U/ml penicillin, 100 µg/ml streptomycin, 0.292 mg/ml L-glutamine (Gibco), 50 µM β-mercaptoethanol (MP Biomedicals), and 1 U/ml rhIL-2 (Roche). Between 2-3 x 10^6 lymphocytes were plated in 24-well tissue culture plates, in the presence or absence of 50 µg/ml rArp (Genscript, or generated in house as previously described [15]). Cultures were incubated for 6-7 days at 37 degrees and 5% CO_2. Every 2-3 days, cultures were spun down at 400 *xg* for 5 minutes, half the culture media was

removed and replaced with fresh media containing 2 U/ml rhIL-2. At the end of the culture period, cells were layered over Ficoll-Paque PLUS (Cytiva) density gradient, and spun at 600 *xg* for 20 minutes at room temperature with no brake to separate out dead cells. The interface layer was collected and washed twice with staining media prior to labeling for flow cytometry.

3.5 References

1. Steere AC, Strle F, Wormser GP, Hu LT, Branda JA, Hovius JW, Li X, Mead PS: **Lyme borreliosis**. *Nat Rev Dis Primers* 2016, **2**:16090.
2. Bunikis J, Tsao J, Luke CJ, Luna MG, Fish D, Barbour AG: **Borrelia burgdorferi Infection in a Natural Population of Peromyscus Leucopus Mice: A Longitudinal Study in an Area Where Lyme Borreliosis Is Highly Endemic**. *The Journal of Infectious Diseases* 2004, **189**:1515-1523.
3. Tilly K, Rosa PA, Stewart PE: **Biology of Infection with Borrelia burgdorferi**. *Infectious Disease Clinics of North America* 2008, **22**:217-234.
4. Rollend L, Fish D, Childs JE: **Transovarial transmission of Borrelia spirochetes by Ixodes scapularis: A summary of the literature and recent observations**. *Ticks and Tick-borne Diseases* 2013, **4**:46-51.
5. Tracy KE, Baumgarth N: **Borrelia burgdorferi Manipulates Innate and Adaptive Immunity to Establish Persistence in Rodent Reservoir Hosts**. *Front Immunol* 2017, **8**:116.
6. Elsner RA, Hastey CJ, Olsen KJ, Baumgarth N: **Suppression of Long-Lived Humoral Immunity Following Borrelia burgdorferi Infection**. *PLoS Pathog* 2015, **11**:e1004976.
7. Xu Q, Seemanapalli SV, McShan K, Liang FT: **Constitutive Expression of Outer Surface Protein C Diminishes the Ability of Borrelia burgdorferi To Evade Specific Humoral Immunity**. *Infection and Immunity* 2006, **74**:5177-5184.
8. Bankhead T, Chaconas G: **The role of VlsE antigenic variation in the Lyme disease spirochete: persistence through a mechanism that differs from other pathogens**. *Molecular Microbiology* 2007, **65**:1547-1558.
9. Lone AG, Bankhead T: **The Borrelia burgdorferi VlsE Lipoprotein Prevents Antibody Binding to an Arthritis-Related Surface Antigen**. *Cell Reports* 2020, **30**:3663-3670.e3665.
10. Hodzic E, Feng S, Freet KJ, Borjesson DL, Barthold SW: **Borrelia burgdorferi population kinetics and selected gene expression at the host-vector interface**. *Infect Immun* 2002, **70**:3382-3388.
11. Hodzic E, Feng S, Freet KJ, Barthold SW: **Borrelia burgdorferi population dynamics and prototype gene expression during infection of immunocompetent and immunodeficient mice**. *Infect Immun* 2003, **71**:5042-5055.
12. Imai D, Holden K, Velazquez EM, Feng S, Hodzic E, Barthold SW: **Influence of arthritis-related protein (BBF01) on infectivity of Borrelia burgdorferi B31**. *BMC Microbiol* 2013, **13**:100.
13. Feng S, Hodzic E, Barthold SW: **Lyme arthritis resolution with antiserum to a 37-kilodalton Borrelia burgdorferi protein**. *Infect Immun* 2000, **68**:4169-4173.
14. Feng S, Hodzic E, Freet K, Barthold SW: **Immunogenicity of Borrelia burgdorferi arthritis-related protein**. *Infect Immun* 2003, **71**:7211-7214.
15. Tunev SS, Hastey CJ, Hodzic E, Feng S, Barthold SW, Baumgarth N: **Lymphoadenopathy during lyme borreliosis is caused by spirochete migration-induced specific B cell activation**. *PLoS Pathog* 2011, **7**:e1002066.
16. Elsner RA, Hastey CJ, Baumgarth N: **CD4+ T cells promote antibody production but not sustained affinity maturation during Borrelia burgdorferi infection**. *Infect Immun* 2015, **83**:48-56.
17. Hastey CJ, Elsner RA, Barthold SW, Baumgarth N: **Delays and diversions mark the development of B cell responses to Borrelia burgdorferi infection**. *J Immunol* 2012, **188**:5612-5622.
18. Meyer AL, Trollmo C, Crawford F, Marrack P, Steere AC, Huber BT, Kappler J, Hafler DA: **Direct enumeration of Borrelia-reactive CD4 T cells ex vivo by using MHC class II tetramers**. *Proceedings of the National Academy of Sciences* 2000, **97**:11433-11438.
19. Sette A, Moutaftsi M, Moyron-Quiroz J, McCausland MM, Davies DH, Johnston RJ, Peters B, Rafii-El-Idrissi Benhnia M, Hoffmann J, Su H-P, et al.: **Selective CD4+ T Cell Help for Antibody Responses to a Large Viral Pathogen: Deterministic Linkage of Specificities**. *Immunity* 2008, **28**:847-858.

20. Kang I, Barthold SW, Persing DH, Bockenstedt LK: **T-helper-cell cytokines in the early evolution of murine Lyme arthritis**. *Infection and Immunity* 1997, **65**:3107-3111.
21. Bockenstedt LK, Kang I, Chang C, Persing D, Hayday A, Barthold SW: **CD4+ T Helper 1 Cells Facilitate Regression of Murine Lyme Carditis**. *Infection and Immunity* 2001, **69**:5264-5269.
22. Gross DM, Steere AC, Huber BT: **T helper 1 response is dominant and localized to the synovial fluid in patients with Lyme arthritis**. *J Immunol* 1998, **160**.
23. Sojka DK, Bruniquel D, Schwartz RH, Singh NJ: **IL-2 Secretion by CD4⁺ T Cells In Vivo Is Rapid, Transient, and Influenced by TCR-Specific Competition**. *The Journal of Immunology* 2004, **172**:6136-6143.
24. Zhao C, Davies JD: **A peripheral CD4+ T cell precursor for naive, memory, and regulatory T cells**. *Journal of Experimental Medicine* 2010, **207**:2883-2894.
25. Nepom GT: **MHC class II tetramers**. *Journal of immunology (Baltimore, Md. : 1950)* 2012, **188**:2477-2482.
26. Bacher P, Scheffold A: **Flow-cytometric analysis of rare antigen-specific T cells**. *Cytometry Part A* 2013, **83A**:692-701.
27. Lissina A, Ladell K, Skowera A, Clement M, Edwards E, Seggewiss R, van den Berg HA, Gostick E, Gallagher K, Jones E, et al.: **Protein kinase inhibitors substantially improve the physical detection of T-cells with peptide-MHC tetramers**. *Journal of Immunological Methods* 2009, **340**:11-24.
28. Wooldridge L, Lissina A, Cole DK, Van Den Berg HA, Price DA, Sewell AK: **Tricks with tetramers: how to get the most from multimeric peptide–MHC**. *Immunology* 2009, **126**:147-164.
29. Moon JJ, Chu HH, Pepper M, McSorley SJ, Jameson SC, Kedl Ross M, Jenkins MK: **Naive CD4+ T Cell Frequency Varies for Different Epitopes and Predicts Repertoire Diversity and Response Magnitude**. *Immunity* 2007, **27**:203-213.
30. Goldrath AW, Bevan MJ: **Selecting and maintaining a diverse T-cell repertoire**. *Nature* 1999, **402**:255-262.
31. Lythe G, Molina-París C: **Some deterministic and stochastic mathematical models of naïve T-cell homeostasis**. *Immunol Rev* 2018, **285**:206-217.
32. Clement RL, Daccache J, Mohammed MT, Diallo A, Blazar BR, Kuchroo VK, Lovitch SB, Sharpe AH, Sage PT: **Follicular regulatory T cells control humoral and allergic immunity by restraining early B cell responses**. *Nature Immunology* 2019, **20**:1360-1371.
33. Sage PT, Sharpe AH: **The multifaceted functions of follicular regulatory T cells**. *Current Opinion in Immunology* 2020, **67**:68-74.
34. Rothaeusler K, Baumgarth N: **Evaluation of intranuclear BrdU detection procedures for use in multicolor flow cytometry**. *Cytometry A* 2006, **69**:249-259.

3.6 Tables

Table 3.1

Table 1. *Arp* gene sequence homology

Species	Strain	Geography	Source	OspC Type	Peptide Length	% Amino Acid Identity to N40	Arp gene location	NCBI accession #
B. burgdorferi	N40	New York	*Ixodes scapularis*	E	332 aa	100	lp28-5	WP_010890266.1
B. burgdorferi	64b	New York	Human	B1	332 aa	100	lp28-5	WP_010890266.1
B. burgdorferi	118a	New York	Human	J	332 aa	100	lp28-5	WP_010890266.1
B. burgdorferi	156a	New York	Human	H2	332 aa	100	lp28-5	WP_010890266.1
B. burgdorferi	B31	New York	*Ixodes scapularis*	A	332 aa	100	lp28-1	WP_010890266.1
B. burgdorferi	PAbe	Germany	Human		332 aa	100	lp28-1	WP_010890266.1
B. burgdorferi	JD1	Massachusetts	*Ixodes scapularis*	C1	332 aa	99.1	lp28-4	WP_014540454.1
B. burgdorferi	72a	New York	Human	G	332 aa	92.15	lp36	WP_012665889.1
B. burgdorferi	94a	New York	Human	U1	332 aa	91.84	lp36	WP_012672552.1
B. afzelii	PKo	Germany	Human	--	--	--	--	--
B. garinii	PBr	Denmark	Human	--	--	--	--	--

3.7 Figures

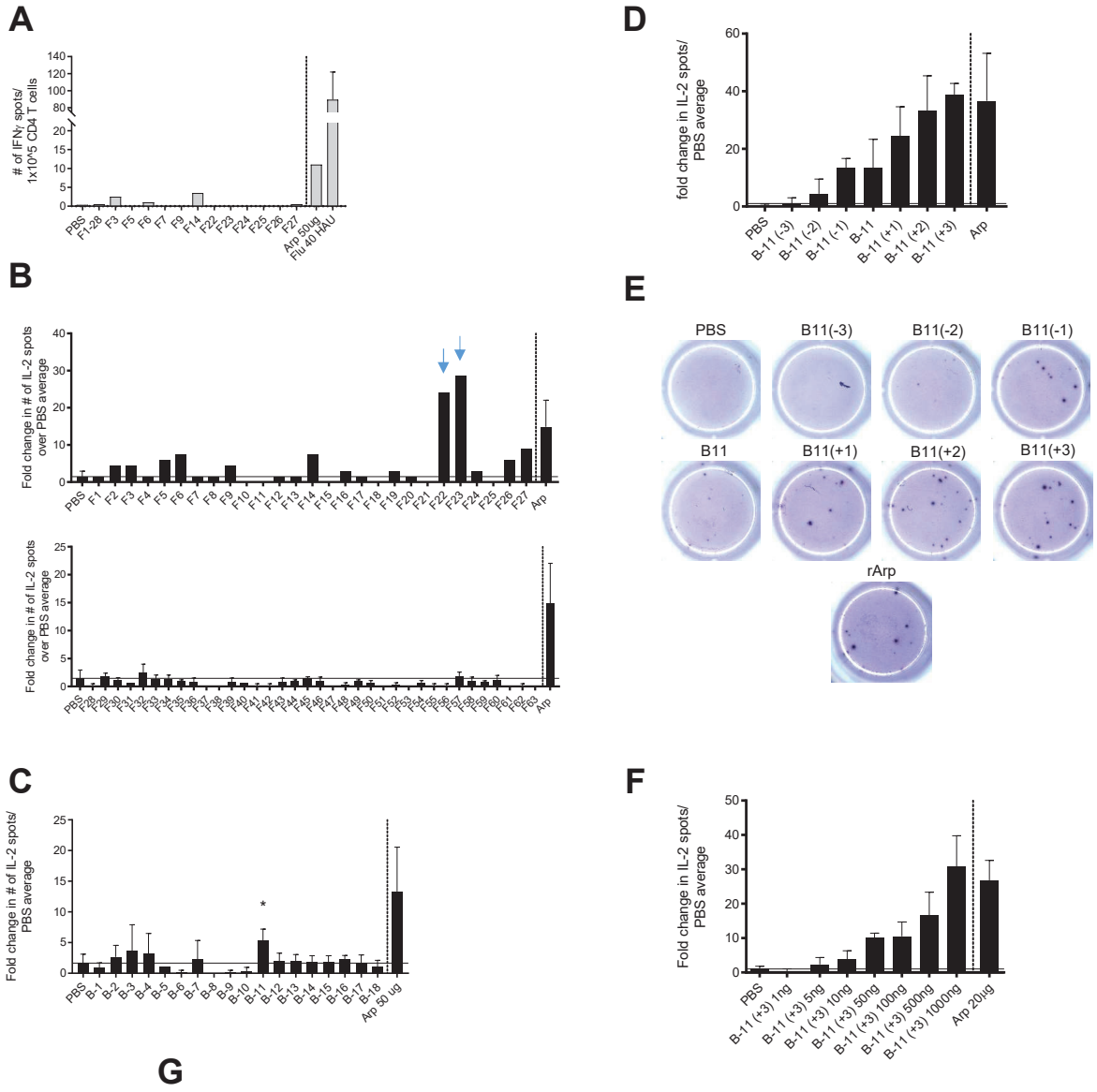

G

MKLLKIFMCAFLLLNLVNCKFDSLNLSTKSVDDKNNSIAKLLQHLSKSEDQANKTSTSED 60

QKELEITENKEQEHEKLSQVAQHAPNSKIEKVKSDGKPVPGDKILSSNKDIYNSYIPEVK 120

EEIVYEILEEVIIPETKIPEITEEVIMPIPQTIDFYIEPRPISSFLTQGTSPSITSTIKS 180

IPQTIDFYIEPRPISSFLTQ F22

DFYIEPRPISSFLTQGTSPS F23

IPQTIDFYIEPRPIS B11

TIDFYIEPRPISSFL $Arp_{152-166}$

YKELAKEKINNGLNIVQKITQNIDNITENLNSKETPKEISGKEVEEKITHPIFDHITGSG 240

NNPGQDSISNTWGEGLEIGGDSNFFTNLEEVRSSIRTKIKVSDGTEQTKDKVEIDEIIED 300

LQKLKEFLEKLKKYLKDTNNLSAIEESVKGLS 332

Figure 3.1: Discovery of an immunodominant Arp epitope. CD4 T cells from Bb infected mice (12 dpi) were stimulated with gene-wide overlapping 20-mer Arp peptides (100 μg per well), recombinant Arp (50 μg per well), or PBS, and analyzed for (**A**) IFNγ or (**B**) IL-2 secretion by ELISPOT. (**A**) CD4 T cells from influenza A/PR8 infected mice (7 dpi) were stimulated with 40 HAU of inactivated virus as a positive control. **(C)** Immunogenic regions identified in (B) were further probed through stimulation with 15-mer Arp peptides B1-B18 and (**D, E**) 15-mer Arp peptides offset by 1 aa residue. Controls were recombinant Arp and PBS. **E)** Representative images of ELISPOT wells. **F)** Peptide-dose response curve of CD4 T cell IL-2 production in response to B11(+3) peptide as assessed by ELISPOT. **G)** Alignment of selected Arp peptide sequences to the whole Arp protein sequence. **A-D**, **F)** Bars represent mean of 2-3 replicate ELISPOT wells ± SD. Data are representative of two (**A, C, D, E, F**) or three (**B**) independent experiments.

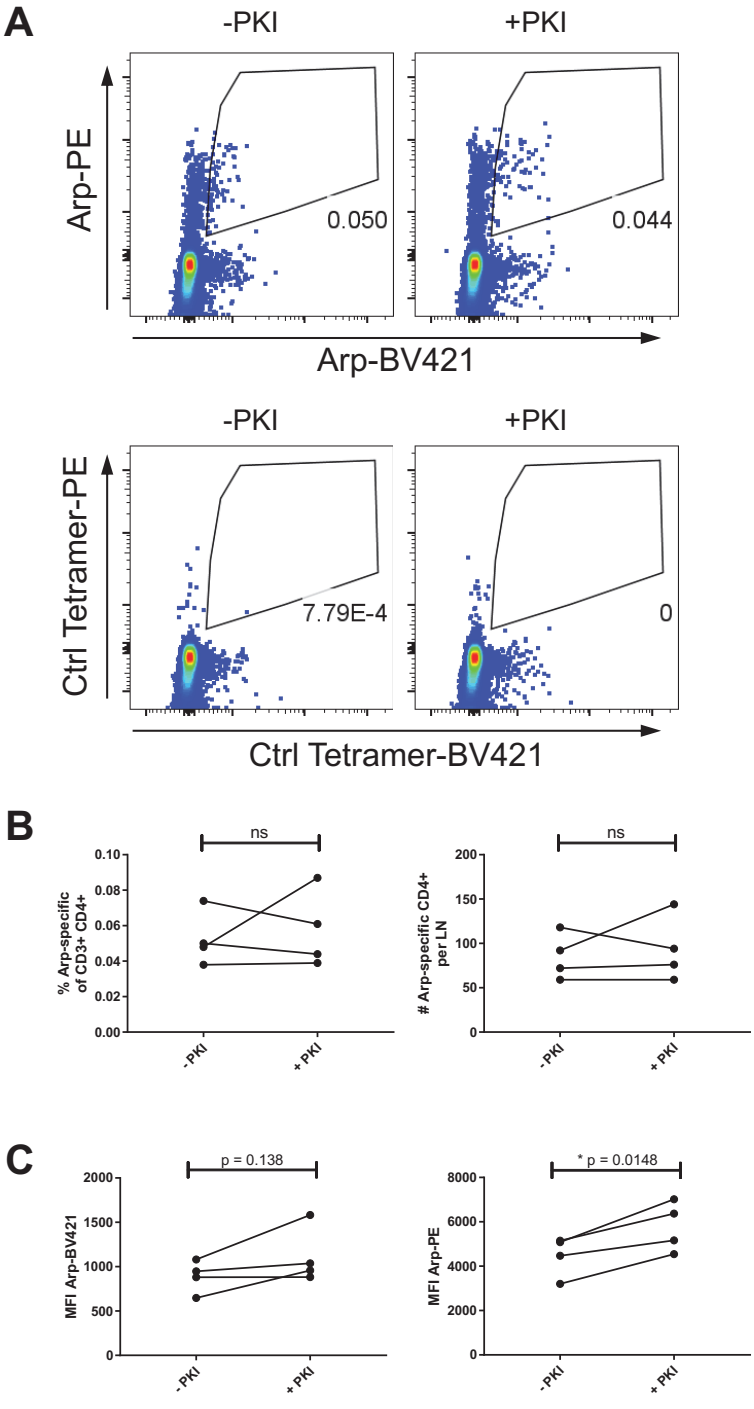
A
-PKI
+PKI
Arp-PE
0.050
0.044
Arp-BV421
-PKI
+PKI
Ctrl Tetramer-PE
7.79E-4
0
Ctrl Tetramer-BV421
B
ns
% Arp-specific of CD3+ CD4+
0.10
0.08
0.06
0.04
0.02
0.00
-PKI
+PKI
ns
Arp-specific CD4+ per LN
200
150
100
50
0
-PKI
+PKI
C
p = 0.138
MFI Arp-BV421
2000
1500
1000
500
0
-PKI
+PKI
* p = 0.0148
MFI Arp-PE
8000
6000
4000
2000
0
-PKI
+PKI

Figure 3.2: PKI treatment improved staining intensity of the Arp$_{152-166}$ tetramers. **A**) Representative FACS plots of draining LN from 14 dpi Bb infected mice. LN cells from individual mice were either treated with a protein kinase inhibitor (+PKI) or incubated in staining media (-PKI) prior to incubation with Arp tetramer. Plots are pre-gated on live single lymphocytes, CD19- CD3+ CD4+. **B**) Frequencies and numbers of Arp-specific CD4 T cells detected in draining LN of 14 dpi Bb infected mice. **C**) Mean fluorescence intensity (MFI) of BV421- and PE-labeled Arp tetramer among CD4+ T cells. N=4 mice, paired two-tailed Student's t-test, *$p<0.05$.

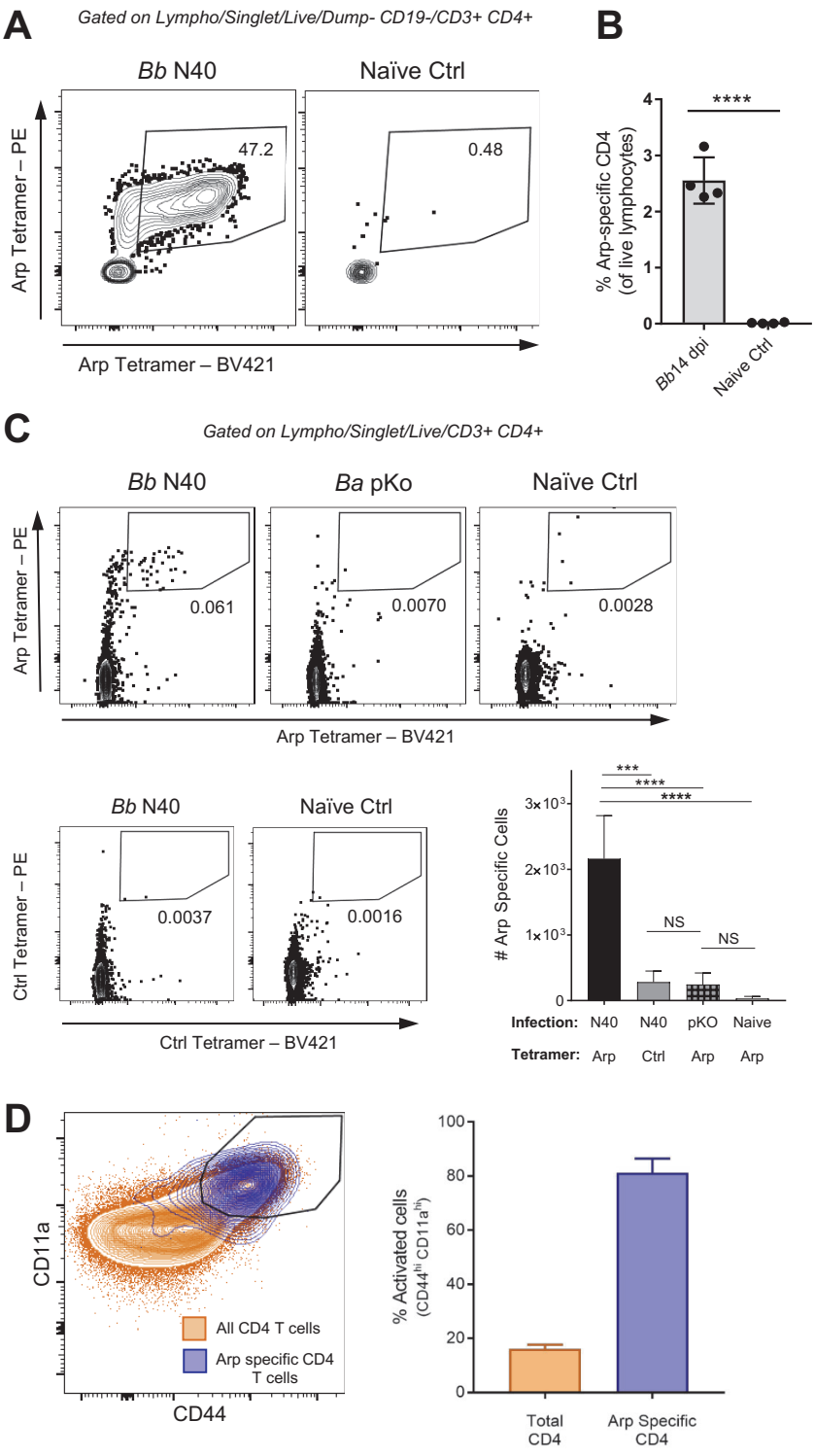
A
Gated on Lympho/Singlet/Live/Dump- CD19-/CD3+ CD4+
Bb N40
Naïve Ctrl
47.2
0.48
Arp Tetramer – PE
Arp Tetramer – BV421
B
% Arp-specific CD4 (of live lymphocytes)
****
Bb14 dpi
Naive Ctrl
C
Gated on Lympho/Singlet/Live/CD3+ CD4+
Bb N40
Ba pKo
Naïve Ctrl
0.061
0.0070
0.0028
Arp Tetramer – PE
Arp Tetramer – BV421
Bb N40
Naïve Ctrl
0.0037
0.0016
Ctrl Tetramer – PE
Ctrl Tetramer – BV421
Arp Specific Cells
***
****
****
NS
NS
Infection: N40 N40 pKO Naive
Tetramer: Arp Ctrl Arp Arp
D
CD11a
CD44
All CD4 T cells
Arp specific CD4 T cells
% Activated cells (CD44hi CD11ahi)
Total CD4
Arp Specific CD4

Figure 3.3: Arp tetramer detects Bb Ag-specific CD4 T cells. **A**) Representative FACS plots show mixed LNs from 14 dpi Bb infected and naïve control mice following enrichment by magnetic pull down of tetramer-labeled cells. **B**) Frequency of Arp-specific CD4 T cells among enriched fractions of lymphocytes from 14 dpi Bb infected (n=4) and naïve (n=4) mice. Data are representative of three independent experiments. **C**) FACS plots show dual Arp-tetramer-labeling of CD4 T cells from the draining LN 14 dpi Bb N40-infected, *B. afzelii* pKo-infected, or naïve control mice (n=4 mice for each condition). Staining with non-specific control tetramer stains for Bb N40 and naïve mice is shown below. Right bar chart shows summary of results. **D**) Overlay 5% contour plot with outliers of staining for CD44 and CD11a among total and Arp-specific CD3+ CD4+ T cells in the draining LN of 14 dpi Bb N40 infected mice (n=4). Bar chart shows summary of activated $CD44^{hi}$ $CD11a^{hi}$ cells ± SD **B**) Two-tailed Student's t-test; **C**) One-way ANOVA with Tukey's post-hoc comparison. ***p<0.001, ****p<0.0001.

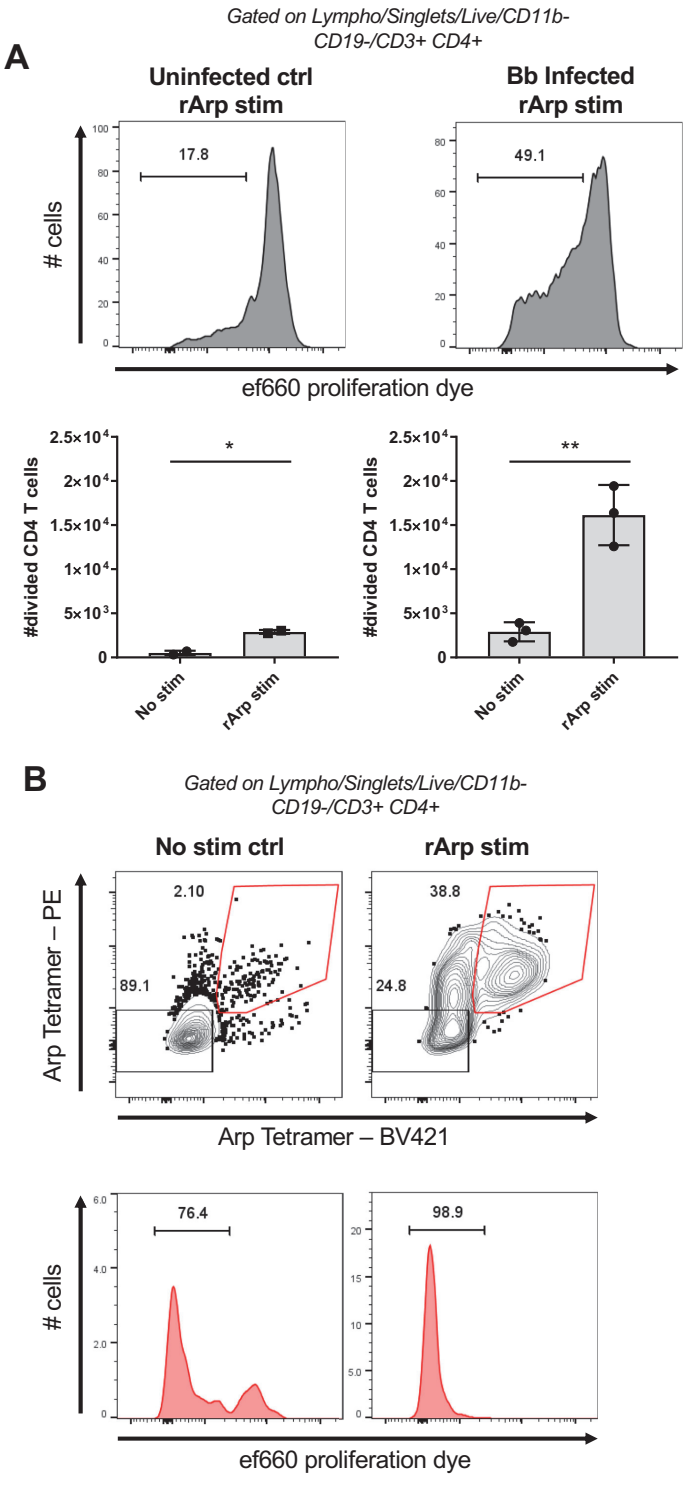
A
Gated on Lympho/Singlets/Live/CD11b-
CD19-/CD3+ CD4+
Uninfected ctrl
rArp stim
Bb Infected
rArp stim
17.8
49.1
cells
ef660 proliferation dye
#divided CD4 T cells
*
**
No stim
rArp stim
B
Gated on Lympho/Singlets/Live/CD11b-
CD19-/CD3+ CD4+
No stim ctrl
rArp stim
2.10
89.1
38.8
24.8
Arp Tetramer – PE
Arp Tetramer – BV421
76.4
98.9
cells
ef660 proliferation dye

Figure 3.4: Arp tetramer binds specifically to rArp stimulated CD4 T cells. A) LN cells from 21 day Bb infected mice or uninfected controls were labeled with proliferation dye, and cultured for 6 days in the presence or absence of rArp protein. Cultures were analyzed via FACS for dilution of proliferation dye (representative FACS plots, top) and total divided CD4 T cells (summary data, bottom). Student's t-test; *= $p<0.05$, **= $p<0.01$. **B)** Draining LN cells from Bb infected mice (21 dpi) were labeled with proliferation dye, and cultured in the presence or absence of rArp protein. After 7 days of culture, similarly treated wells were pooled, labeled with $Arp_{152-166}$ tetramers, and $Arp_{152-166}$ specific cells (top panels) were analyzed for proliferation via FACS (bottom panels).

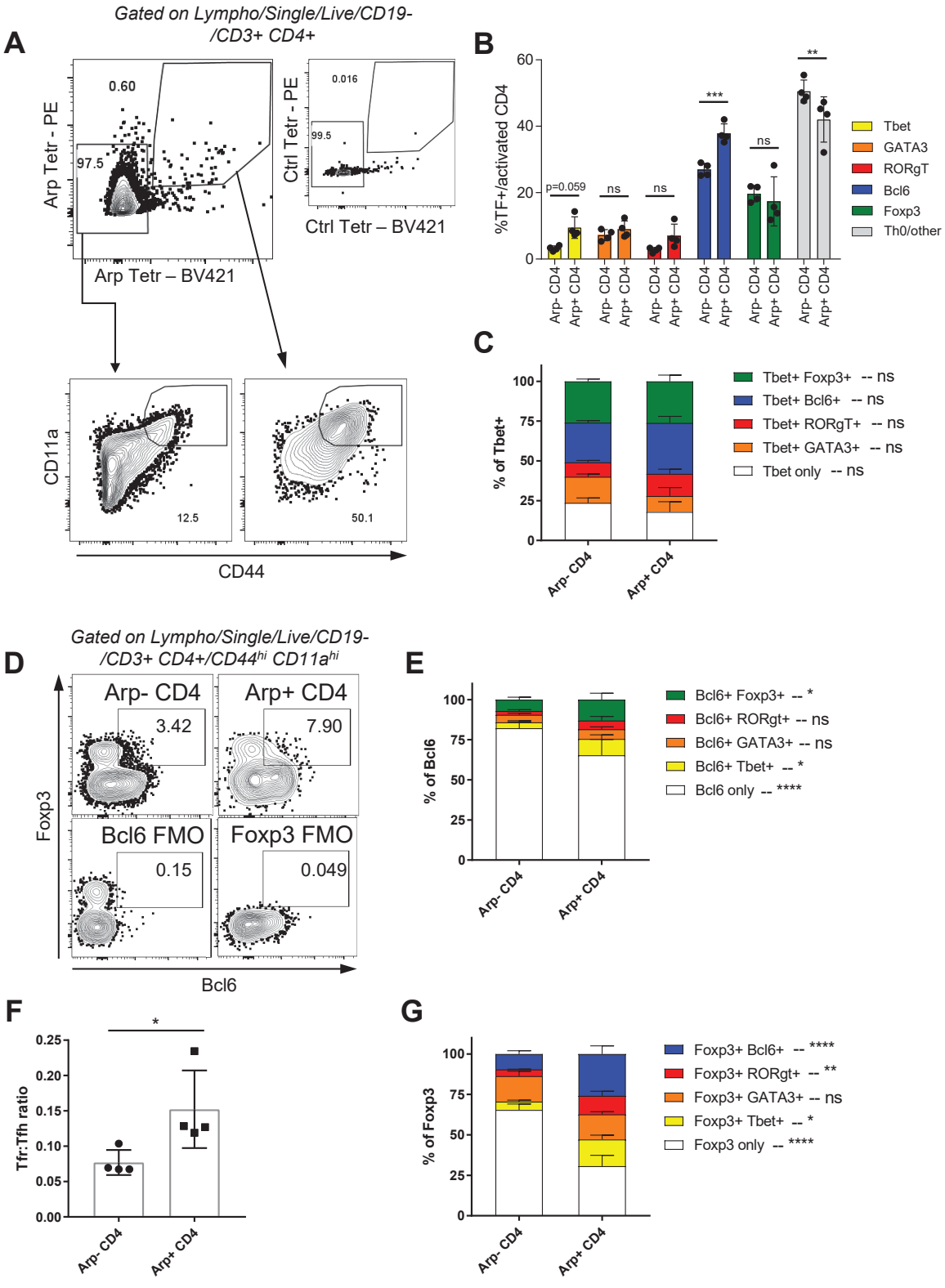
A
Gated on Lympho/Single/Live/CD19-/CD3+ CD4+
Arp Tetr - PE
Arp Tetr – BV421
0.60
97.5
Ctrl Tetr - PE
Ctrl Tetr – BV421
0.016
99.5
CD11a
CD44
12.5
50.1
B
%TF+/activated CD4
p=0.059
ns
***
**
Arp- CD4
Arp+ CD4
Tbet
GATA3
RORgT
Bcl6
Foxp3
Th0/other
C
% of Tbet+
Tbet+ Foxp3+ -- ns
Tbet+ Bcl6+ -- ns
Tbet+ RORgT+ -- ns
Tbet+ GATA3+ -- ns
Tbet only -- ns
D
Gated on Lympho/Single/Live/CD19-/CD3+ CD4+/CD44hi CD11ahi
Arp- CD4
Arp+ CD4
3.42
7.90
Bcl6 FMO
Foxp3 FMO
0.15
0.049
Foxp3
Bcl6
E
% of Bcl6
Bcl6+ Foxp3+ -- *
Bcl6+ RORgt+ -- ns
Bcl6+ GATA3+ -- ns
Bcl6+ Tbet+ -- *
Bcl6 only -- ****
F
Tfr:Tfh ratio
*
G
% of Foxp3
Foxp3+ Bcl6+ -- ****
Foxp3+ RORgt+ -- **
Foxp3+ GATA3+ -- ns
Foxp3+ Tbet+ -- *
Foxp3 only -- ****

Figure 3.5: Arp-specific CD4 T cells are enriched for Bcl6+ Tfh. A) The draining LNs of Bb infected mice were harvested 14 dpi, and processed and labeled for FACS analysis. **B)** Highly activated Arp-specific (Arp+) CD4 T cells and non-tetramer binding cells (Arp-) were analyzed for expression of lineage defining transcription factors. **C)** Tbet-expressing CD4 T cells were analyzed for co-expression of additional lineage-defining transcription factors. **D)** Representative FACS plots of Bcl6 and Foxp3 coexpression in Arp+ and Arp- CD4 T cells. FMO controls are shown below. **E)** Bcl6-expressing CD4 T cells were analyzed for co-expression of additional lineage-defining transcription factors. **F)** The ratio of Tfr (Foxp3+ Bcl6+) to Tfh (Foxp3- Bcl6+) cells was calculated for Arp+ and Arp- CD4 T cells. **G)** Foxp3-expressing CD4 T cells were analyzed for co-expression of additional lineage-defining transcription factors. N=4 mice, representative of three independent experiments. Statistical analysis for **B-C)**, **E)** and **G)** is 2-way ANOVA with Sidak's multiple comparison correction. **F)** is paired student's t-test.

Conclusion

Although it is well established that B cell immunity to *Borrelia burgdorferi* (Bb) infection is critical for host defense, the role of CD4 T cells in host defense against this pathogen remains enigmatic. Since CD4 T cells are an indispensable component of host defense against microbial pathogens, it stands to reason that they also play an important role in defense against Bb infection. To date, however, most studies on CD4 T cell responses to Bb infection have focused on their role in inducing host pathology (see **Chapter 1**, or [1]). They provided little evidence that CD4 T cells play a role in host protection [2]. I therefore set out to reexamine the extent to which CD4 T cells either contribute, or fail to contribute, toward host defense against Bb.

One particular aspect of the CD4 response I focused on was T cell polarization (**Chapter 2**). Although Bb is an extracellular bacterium, it has been widely reported and it is generally accepted that Bb induces a Th1 dominant CD4 T cell response [3,4]. Since most of the work done to establish that Bb induces a Th1 response occurred prior to the discovery and characterization of additional CD4 T cell polarization states, such as Th17 and Tfh, I reasoned that it would be useful to reassess Bb induced CD4 T cell polarization using several approaches, and to assess the degree of CD4 T cell polarization towards the following major CD4 T cell subsets: Th1, Th2, Th17 (effector T cells), Tfh (B cell helper T cells), and Treg (regulatory T cells). First, I conducted qRT-PCR to measure the induction of mRNA transcripts of lineage defining cytokines and transcription factors in highly purified populations of CD4 T cells from the draining LNs of Bb infected mice. Although I found that the Th1-associated transcription factor *Tbx21* was more highly upregulated than Th2- or Th17-associated transcription factors, *Tbx21* induction appeared weak and transient, returning to baseline levels by 14 dpi (**Figure 2.2**). Surprisingly, the Th1 cytokine *Ifng* was not significantly increased over baseline levels (**Figure 2.2**). When I assessed CD4 T cell polarization via multi-color flow cytometry, I observed a similarly weak Th1 polarization assessed via staining for Tbet, encoded by the master transcriptional regulator of Th1 polarization, Tbx21 (**Figure 2.3**). Nevertheless,

induction of Th1 lineage markers was greater than induction of Th2 or Th17 markers, consistent with previous literature.

Since effector T cells are able to exit the LN and migrate to sites of inflammation in the tissues, I also analyzed the polarization state of CD4 T cells at an important effector site in Bb infection, the skin, as T cell polarization may require time from initial induction in the LN and/or environmental cues from an effector site. Somewhat surprisingly, CD4 T cell polarization to effector subsets in the skin was not observed above that seen in the LN (**Figures 2.5** and **2.6**). We also tested the possibility that effector polarization might increase at late timepoints of Bb infection, and found that effector CD4 polarization remained minimal over the course of infection (**Figure 2.6**). Although it appears that Bb infection results in greater Th1 polarization compared to either Th2 or Th17 polarization, together our data suggests overall weak or incomplete effector T cell polarization.

One technical limitation of the studies outlined above is that they could not distinguish antigen (Ag) specific CD4 T cells from polyclonal T cells that may have undergone bystander activation during Bb infection. Therefore, we set out to generate a system in which we could identify Bb-specific CD4 T cells. We did this by conducting a comprehensive epitope mapping study to identify an immunoreactive epitope on the T-dependent Bb surface antigen, Arthritis related protein (Arp) (**Chapter 3**). Notably, during this screen we discovered that we could not detect IFNγ secretion by *ex vivo* Arp peptide stimulated CD4 T cells from day 10 Bb infected mice (**Figure 3.1**), consistent with my mRNA analysis that failed to demonstrate significant *Ifng* induction (**Figure 2.2**). Using the newly identified Arp epitope, we developed a pMHCII tetramer that was capable of identifying Arp-specific CD4 T cells (**Figures 3.3** and **3.4**). Using this novel tetramer reagent, I assessed the polarization state of Ag-specific CD4 T cells alongside polyclonal CD4 T cells, and found that Arp-specific CD4 T cells exhibited similarly weak Th1

polarization as polyclonal effector T cells (**Figure 3.5**). These results help support my earlier conclusions that Bb induces a weak effector response, characterized by slight Th1 skewing.

Our lab previously described that Bb infection induces lymphadenopathy, characterized by a highly disorganized LN architecture [5,6]. We hypothesized then that the dis-coordinated nature of the LN response might lead to impairment of the quality of B cell responses. Given my data, it stands to reason that the induction of optimal CD4 T cell responses may be similarly impaired, which may be manifested in a lack of T cell polarization. Although early type I IFNg induction has been implicated in driving aspects of the dysregulated B cell response to Bb infection [7], it is not known whether this mechanism, or others, contributes to suboptimal CD4 T cell polarization.

Another important unresolved question is what role Th1 dominant polarization of effector CD4 T cells plays in host immunity to Bb. Although there is a well-established correlation between the production of the hallmark Th1 cytokine IFNγ and the severity of certain Lyme disease pathologies such as Lyme arthritis [8], it is less clear whether Th1 responses play a role in limiting bacterial replication and dissemination. Although increased IFNγ was correlated with decreased bacterial burden in certain mouse models [9-11], it is not clear whether this effect is T cell intrinsic. Furthermore, our data indicated little to no production of IFNγ by CD4 T cells in response to Bb infection. Further studies are warranted to understand whether Th1 polarization, and whether CD4 T cell derived IFNγ, contributes to host protection against Bb infection.

One possibility that should be considered in future studies of CD4 responses to Bb is that polarization of effector CD4 T cells towards a subset other than Th1 may be beneficial to host protection. For instance, a Th17 dominated response to Bb could potentially be more effective than a Th1 driven response, since

Th17 responses are particularly well-suited to combatting extracellular bacterial infections [12]. One major function of Th17 cells is mobilization and recruitment of neutrophils via production of IL-17 [13], and neutrophils have previously been shown to be beneficial to host protection against Bb infection [14]. Furthermore, type I IFN has been shown to impair Th17 mediated neutrophil recruitment and host protection against secondary bacterial pneumonia following influenza infection [15,16]. Since Bb induces strong type I IFN signaling [4], it is unsurprising that stronger Th1 polarization is induced compared to Th17. Furthermore, previous studies established that *Tbx21* expression suppresses the induction of *Rorc*, the transcriptional regulator of Th17 polarization [17], thus Th1 polarization also directly inhibits the development of Th17 effectors. If Th17 polarization is indeed suppressed during Bb infection, this may limit neutrophil mobilization and impair neutrophil mediated control of Bb. Indeed histological evaluation of Bb-infected mouse tissues showed little evidence for a granulocytic infiltrate by about day 7 following infection [14], a finding confirmed by us via flow cytometry (data not shown), further supporting the idea that a lack of local IL17 production may inhibit effective innate immune response activation during Bb infection, helping the spirochetes to evade clearance.

In several preliminary experiments, I tested whether administration of rIL-17 to Bb infected mice improved neutrophil mobilization to the skin, as well as control of bacterial burden. Although greater numbers of neutrophils were seen circulating in mice treated with rIL-17, I did not observe enhanced neutrophil infiltration of the skin (data not shown). Additionally, rIL-17 treatment did not significantly affect bacterial burden in the skin, or in other tissues (data not shown). Although treatment with the hallmark Th17 cytokine IL-17 did not appear to benefit host defense in these experiments, it is possible that the cytokine treatment was insufficient in dose or frequency. Thus, further investigation into the efficacy of Th17 responses in host defense against Bb is warranted.

In contrast to the weak effector polarization that was observed in response to Bb infection, I consistently observed robust induction of the lineage defining Tfh transcription factor Bcl6 among LN CD4 T cells (**Figures 2.2** and **2.3**). T cells identified as specific for Arp were even more likely to express the Tfh defining transcription factor Bcl6 than polyclonal cells (**Figure 3.5**), which supported previous studies from our lab that had previously observed strong T-dependent Arp-specific IgG responses in C57BL/6 mice [18]. Intriguingly, Arp-specific CD4 T cells were more likely than polyclonal cells to co-express Foxp3 with Bcl6, indicative of greater induction of Arp-specific Tfr cells (**Figure 3.5**). Although greater numbers of Arp-specific Tfr might indicate tighter regulation of the Arp-specific humoral response, the functional consequences of this observation require further exploration, given that we observed the presence of Arp-specific germinal center B cells at days 14 and 21 after infection, but not at day 28 (data not shown.

In light of the strong induction of Tfh responses, it is important to further investigate role of Tfh in the GC response to Bb infection. Our lab has previously identified significant defects in Bb induced GC responses, including a lack of long lived plasma cell formation, defects in affinity maturation, and premature GC collapse [6,19]. Thus it will be important in the future to identify whether the population of Bcl6+ Tfh are fully functional and/or whether the presence of Tfr might suppress the response. Although I observed strong upregulation of *Il21* transcripts in LN CD4 T cells (**Figure 2.2**), suggesting their ability to produce the hallmark Tfh cytokine IL-21, it will be important to examine additional functional aspects of the Tfh generated in response to Bb infection. Indeed, our lab previously showed that CD4 T cells from Bb infected mice had altered functionality in driving T-dependent B cell responses, favoring rapid plasma cell differentiation rather than B cell proliferation [18]. Identification of Bb-induced functional changes to Tfh could help explain why the GC response fails to induce effective B cell immunity to Bb, and why Bb is able to persist in spite of a robust Ab response.

In summary, my data provide evidence that CD4 T cells undergo weak effector polarization in response to Bb infection. Ineffective induction, or alterations of CD4 T cell effector polarization may constitute a previously overlooked but potentially powerful aspect of Bb-mediated immune evasion that identifies CD4 T cells as a potential target of Bb-mediated immune suppression. My data also show that, relative to the weak induction of effector subsets, Tfh are strongly induced, but that a relatively high frequency express a regulatory phenotype. Additionally, I have described the development and validation of a novel reagent to identify CD4 T cells specific for the highly conserved and T-dependent Bb surface antigen Arp will provide a critical reagent to further explore the function of CD4 T cells in Bb infection.

4.1 References

1. Hammond EM, Baumgarth N: **CD4 T cell responses in persistent Borrelia burgdorferi infection**. *Current Opinion in Immunology* 2022, **77**:102187.
2. Fikrig E, Barthold SW, Chen M, Chang CH, Flavell RA: **Protective antibodies develop, and murine Lyme arthritis regresses, in the absence of MHC class II and CD4+ T cells**. *The Journal of Immunology* 1997, **159**:5682-5686.
3. Bockenstedt LK, Kang I, Chang C, Persing D, Hayday A, Barthold SW: **CD4+ T Helper 1 Cells Facilitate Regression of Murine Lyme Carditis**. *Infection and Immunity* 2001, **69**:5264-5269.
4. Miller JC, Ma Y, Bian J, Sheehan KC, Zachary JF, Weis JH, Schreiber RD, Weis JJ: **A critical role for type I IFN in arthritis development following Borrelia burgdorferi infection of mice**. *J Immunol* 2008, **181**.
5. Tunev SS, Hastey CJ, Hodzic E, Feng S, Barthold SW, Baumgarth N: **Lymphoadenopathy during lyme borreliosis is caused by spirochete migration-induced specific B cell activation**. *PLoS Pathog* 2011, **7**:e1002066.
6. Hastey CJ, Elsner RA, Barthold SW, Baumgarth N: **Delays and diversions mark the development of B cell responses to Borrelia burgdorferi infection**. *J Immunol* 2012, **188**:5612-5622.
7. Hastey CJ, Ochoa J, Olsen KJ, Barthold SW, Baumgarth N: **MyD88- and TRIF-independent induction of type I interferon drives naive B cell accumulation but not loss of lymph node architecture in Lyme disease**. *Infect Immun* 2014, **82**:1548-1558.
8. Lochhead RB, Strle K, Arvikar SL, Weis JJ, Steere AC: **Lyme arthritis: linking infection, inflammation and autoimmunity**. *Nature Reviews Rheumatology* 2021, **17**:449-461.
9. Brown JP, Zachary JF, Teuscher C, Weis JJ, Wooten RM: **Dual Role of Interleukin-10 in Murine Lyme Disease: Regulation of Arthritis Severity and Host Defense**. *Infection and Immunity* 1999, **67**:5142-5150.
10. Siebers EM, Liedhegner ES, Lawlor MW, Schell RF, Nardelli DT, Raffatellu M: **Regulatory T Cells Contribute to Resistance against Lyme Arthritis**. *Infection and Immunity* 2020, **88**:e00160-00120.
11. Anguita J, Persing DH, Rincon M, Barthold SW, Fikrig E: **Effect of anti-interleukin 12 treatment on murine lyme borreliosis**. *The Journal of Clinical Investigation* 1996, **97**:1028-1034.
12. Peck A, Mellins Elizabeth D: **Precarious Balance: Th17 Cells in Host Defense**. *Infection and Immunity* 2010, **78**:32-38.
13. Curtis MM, Way SS: **Interleukin-17 in host defence against bacterial, mycobacterial and fungal pathogens**. *Immunology* 2009, **126**:177-185.
14. Xu Q, Seemanapalli SV, Reif KE, Brown CR, Liang FT: **Increasing the Recruitment of Neutrophils to the Site of Infection Dramatically Attenuates *Borrelia burgdorferi* Infectivity**. *The Journal of Immunology* 2007, **178**:5109-5115.
15. Kudva A, Scheller EV, Robinson KM, Crowe CR, Choi SM, Slight SR, Khader SA, Dubin PJ, Enelow RI, Kolls JK, et al.: **Influenza A inhibits Th17-mediated host defense against bacterial pneumonia in mice**. *J Immunol* 2011, **186**:1666-1674.
16. Shepardson Kelly M, Larson K, Morton Rachelle V, Prigge Justin R, Schmidt Edward E, Huber Victor C, Rynda-Apple A: **Differential Type I Interferon Signaling Is a Master Regulator of Susceptibility to Postinfluenza Bacterial Superinfection**. *mBio* 2016, **7**:e00506-00516.
17. Gökmen MR, Dong R, Kanhere A, Powell N, Perucha E, Jackson I, Howard JK, Hernandez-Fuentes M, Jenner RG, Lord GM: **Genome-Wide Regulatory Analysis Reveals That T-bet Controls Th17 Lineage Differentiation through Direct Suppression of IRF4**. *The Journal of Immunology* 2013, **191**:5925-5932.

18. Elsner RA, Hastey CJ, Baumgarth N: **CD4+ T cells promote antibody production but not sustained affinity maturation during Borrelia burgdorferi infection**. *Infect Immun* 2015, **83**:48-56.
19. Elsner RA, Hastey CJ, Olsen KJ, Baumgarth N: **Suppression of Long-Lived Humoral Immunity Following Borrelia burgdorferi Infection**. *PLoS Pathog* 2015, **11**:e1004976.